



Supporting Information

Bismuth Amides Mediate Facile and Highly Selective Pn–Pn Radical-Coupling Reactions (Pn = N, P, As)

*Kai Oberdorf, Anna Hanft, Jacqueline Ramler, Ivo Krummenacher, F. Matthias Bickelhaupt,
Jordi Poater,* and Crispin Lichtenberg**

[anie_202015514_sm_miscellaneous_information.pdf](#)

SUPPORTING INFORMATION

Table of Contents

Experimental.....	3
Single Crystal X-ray Analysis.....	5
Literature-Known Bismuth Amides.....	7
Reaction monitoring: Formation of Compounds 3-X from 1-Me.....	8
Kinetic Investigations of Formation of 3-Me from 1-Me.....	9
NMR Spectroscopic data of the hydrazine derivatives 3-X.....	11
Reactivity of secondary pnictogens towards bismuth amides.....	12
EPR Spectroscopic Measurements.....	14
NMR Spectra of Isolated Compounds.....	15
Quantum Chemical Analyses	23
References.....	43
Author Contributions.....	43
Conflict of Interest.....	43
Acknowledgements.....	43

SUPPORTING INFORMATION**Experimental****General considerations**

All air and moisture-sensitive manipulations were carried out using standard Schlenk techniques or in a glovebox containing purified argon. Solvents were purified by distillation using the appropriate drying agents, degassed and stored over molecular sieves (4 Å) prior to use. Deuterated solvents used for NMR spectroscopy were dried, degassed and stored over molecular sieves (4 Å) under dry argon prior to use. Bis(4-trifluoromethylphenyl)amine,^[1] Bi(NMe₂)₃ (**4**),^[2] bis(4-trifluoromethylphenyl)phosphane,^[3] bis(4-methoxyphenyl)phosphane,^[4] bis(4-chlorophenyl)phosphane^[4] and diphenylarsane^[5] were synthesized according to the literature. BiCl₃ was sublimed prior to use.

All NMR spectra were acquired either on a Bruker Avance 400 spectrometer or on a Bruker Avance I 500 spectrometer. ¹H and ¹³C chemical shifts are reported relative to SiMe₄ using the residual solvent peak of the solvent as secondary standard. ¹⁹F chemical shifts are reported relative to CFCl₃ as an external standard. ¹⁵N chemical shifts are reported relative to CH₃NO₂ (90% in CDCl₃) and were determined by two-dimensional ¹H-¹⁵N correlation NMR spectroscopic experiments. Elemental analyses (C, H, N, S) were conducted on a Vario Micro Cube by Elementar Analysesysteme GmbH. Reproducibly satisfactory elemental analyses of **1-CF₃** and **1-OMe** proved to be difficult to obtain, which was ascribed to the air and temperature sensitivity of the compounds. In order to provide evidence for the efficacy of the synthesis of these compounds, the bismuth content of **1-CF₃** and **1-OMe** was determined by complexometric titrations according to previously reported procedures using a solution of the disodium salt of ethylenediaminetetraacetic acid as a titrant and Xylenol Orange as an indicator. For mass spectrometric analyses, an Exactive plus instrument (Thermo Scientific) was used.

Single-crystals suitable for X-ray diffraction analysis were coated with perfluorinated polyether oil in a glovebox, transferred to a nylon loop and then transferred to the goniometer of a diffractometer (Bruker D8 Quest or Bruker X8-Apex II) equipped with a molybdenum X-ray tube ($\lambda = 0.71073 \text{ \AA}$).

EPR measurements at X-band were carried out at ambient temperature using a Bruker ELEXSYS E580 CW/FT EPR spectrometer. The spectral simulations were performed using MATLAB 9.6 (2019a) and the EasySpin 5.2.25 toolbox.^[6]

Discussion

In the original procedure, compound **1-H** was purified by re-crystallization from CH₂Cl₂ over a period of days, resulting in an isolated yield of 30% (the reported ¹³C NMR spectrum showed signals of the hydrazine Ph₄N₂ (**3-H**), which were not identified as such).^[7] Our procedure avoids the use of CH₂Cl₂ which was confirmed as one cause of decomposition. Keeping **1-H** in solution for extended periods of time was avoided because it also favors the decomposition of **1-H**. In combination, these modifications resulted in 88% yield of analytically pure material (route 1). Compounds **1-Me** and **1-OMe** were obtained in an analogous approach, albeit with somewhat lower yields of 79% and 51%, respectively. The reduced yields were ascribed to the high reactivity of compounds **1-Me** and **1-OMe** in solution (see main part). For other derivatives of **1-H**, different synthetic approaches were required. In the case of **1-Br** and **1-Ph** this is due to limited solubility of the amines. Also, route 1 does not give quantitative conversion of the *in situ* generated lithium amides to the bismuth compounds in these cases. As an alternative route, a salt elimination reaction of the potassium amides (generated *in situ* from KH and the respective amine) and BiI₃ was established (route 2). Due to the sufficiently poor solubility of KI in THF, the reaction can be carried out in THF and the by-product KI can be filtered off without changing to another solvent system. The products **1-Ph** and **1-Br** were obtained in 87% and 83% yield by precipitation through addition of pentane. The use of this method for **1-OMe** improved the yield from 51% to 78% which highlights the advantage of route 2. Routes 1 and 2 are not as easily feasible for **1-CF₃** due to the lability of the lithium or potassium amides at temperatures above -78 °C. Rapid decomposition of these species was observed. A mild transamination reaction of Bi(NMe₂)₃ (**4**) with the amine HN(4-CF₃-C₆H₄)₂ was successful in this case. This required extended reaction times, but was facilitated by the stability of **1-CF₃** in solution.

[Bi(NPh₂)₃] (1-H). The synthesis was conducted according to an optimized procedure based on the synthesis published by Clegg et al..^[7] Diphenylamine (2.42 g, 14.3 mmol) was dissolved in THF (15 mL) and cooled to 0 °C. A solution of *n*-BuLi in hexanes (8.9 mL, 1.6 M, 14.3 mmol) was added dropwise. The reaction mixture turned yellow and was stirred at ambient temperature for 90 min. BiCl₃ (1.50 g, 4.80 mmol) was dissolved in THF (15 mL) and cooled to 0 °C. The yellow amide solution was slowly transferred to the BiCl₃ solution with an immediate color change to orange. After completion of the addition, the reaction mixture was warmed to ambient temperature and stirred for 30 min followed by removal of the solvent under reduced pressure. The orange residue was dissolved in benzene (5 mL) and filtered over celite. The solvent was removed under reduced pressure and the residue was washed with pentane (3 × 5 mL). The orange powder was dried *in vacuo* for 3 h.

Yield: 3.01 g (4.22 mmol, 88%)

¹H NMR: (298 K, 400 MHz, Benzene-*d*₆): $\delta = 6.66 - 6.77$ (m, 18H, 2,4,6-C₆H₅), 7.04 – 7.09 (m, 12H, 3,5-C₆H₅) ppm.

¹³C NMR: (298 K, 100 MHz, Benzene-*d*₆): $\delta = 122.5$ (s, 4-C₆H₅), 124.5 (s, 2,6-C₆H₅), 129.6 (s, 3,5-C₆H₅), 151.3 (s, 1-C₆H₅) ppm.

¹H NMR: (298 K, 400 MHz, Methylenedichloride-*d*₂): $\delta = 6.60$ (dd, 12H, ³J_{HH} = 8.6 Hz, ⁴J_{HH} = 0.93 Hz, 2,6-C₆H₅), 6.86 (t, 6H, ³J_{HH} = 7.4 Hz, 5-C₆H₅) 7.18 (dd, 12 H, ³J_{HH} = 7.4 Hz, ³J_{HH} = 8.5 Hz, 3,5-C₆H₅) ppm.

SUPPORTING INFORMATION

¹³C NMR: (298 K, 100 MHz, Methylenedichloride-*d*₂): δ = 122.7 (s, 4-C₆H₅), 124.5 (s, 2,6-C₆H₅), 129.7 (s, 3,5-C₆H₅), 151.3 (s, 1-C₆H₅) ppm.

Elemental analysis: Anal. calc. for C₃₆H₃₀BiN₃ (713.64 g · mol⁻¹): C, 60.59; H, 4.24; N, 5.89; found: C, 60.48; H, 4.38; N, 5.81.

[Bi[N(4-Me-C₆H₄)₂]₃] (1-Me). Di(*p*-tolyl)amine (3.75 g, 19.0 mmol) was dissolved in THF (9 mL). After cooling to 0 °C, a solution of *n*-BuLi in *n*-hexanes (7.60mL, 2.5 M, 19.0 mmol) was added dropwise. A yellow solution was obtained, which gradually changed its color to deep green while stirring for 1 h at 0 °C. BiCl₃ (2.00 g, 6.34 mmol) was dissolved in THF (9 mL) and cooled to 0 °C. The green amide solution was slowly added resulting in an immediate color change to orange. After completion of the addition, the reaction mixture was stirred for 30 min at 0 °C. All volatiles were removed under reduced pressure. Benzene (10 mL) was added to the residue and an orange suspension with a grey solid was formed. The mixture was filtrated over celite. After removing the solvent under reduced pressure from the filtrate and drying the resulting solid for one hour *in vacuo*, the residue was washed with pentane to give a red powder after drying for 3 h *in vacuo*.

Yield: 3.97 g (4.98 mmol, 79%)

¹H NMR (298 K, 400 MHz, Benzene-*d*₆): δ = 2.16 (s, 18H, C₆H₄Me), 6.76 (d, 12H, ³J_{HH} = 8.3 Hz, 2,6-C₆H₄Me), 6.94 (d, 12H, ³J_{HH} = 8.3 Hz, 3,5-C₆H₄Me) ppm.

¹³C NMR (298 K, 125 MHz, Benzene-*d*₆): δ = 20.6 (s, C₆H₄Me), 124.5 (s, 2,6-C₆H₄Me), 130.1 (s, 3,5-C₆H₄Me), 131.3 (s, 4-C₆H₄Me), 149.4 (s, 1-C₆H₄Me) ppm.

¹⁵N NMR (298 K, 50 Hz, Benzene-*d*₆): δ = -217.1 (s) ppm.

Elemental analysis. Anal. calc. for C₄₂H₄₂BiN₃ (797.32 g · mol⁻¹): C, 63.23; H, 5.31; N, 5.27; found: C, 62.90; H, 5.44; N, 5.08.

[Bi[N(4-MeO-C₆H₆)₂]₃] (1-OMe). 4,4'-Dimethoxydiphenylamine (400 mg, 1.75 mmol) was dissolved in THF (5 mL). After cooling to 0 °C, a solution of *n*-BuLi in *n*-hexanes (1.09 mL, 1.6 M, 1.75 mmol) was added dropwise. A yellow solution was obtained while stirring for 1 h at 0 °C. BiCl₃ (184 mg, 0.58 mmol) was dissolved in THF (5 mL) and cooled to 0 °C. The yellow amide solution was slowly added resulting in an immediate color change to orange. After completion of the addition, the reaction mixture was stirred for 20 min at 0 °C, and all volatiles were removed under reduced pressure. Benzene (5 mL) was added and the orange suspension was filtered over celite. After removing all volatiles from the filtrate under reduced pressure, the residue was washed with pentane to give a brown powder as product after drying for 3 h *in vacuo*.

Yield: 267 mg (0.30 mmol, 51%)

A solution of 4,4'-Dimethoxydiphenylamine (875 mg, 3.82 mmol) in THF (8 mL) was cooled to 0 °C and a dispersion of potassium hydride (154 mg, 3.83 mmol) in THF (2 mL) was slowly added. An immediate gas evolution and a color change to dark green were observed. The solution was allowed to warm to ambient temperature while stirring for 4 h. BiI₃ (750 mg, 1.27 mmol) was dissolved in THF (8 mL) and cooled to -78 °C. The amide solution was slowly added with an immediate color change to red. While warming to around -20 °C a white solid precipitated. After stirring for 10 min, all solids were removed by filtration over celite. The solvent was removed from the filtrate under reduced pressure. The resulting solid was washed with pentane (6 × 5 mL) and dried *in vacuo* for 30 min.

Yield: 882 mg (0.99 mmol, 78%)

¹H NMR (298 K, 500 MHz, Benzene-*d*₆): δ = 3.33 (s, 18H, C₆H₄OMe), 6.77 – 6.82 (m, 24H, 2,3,5,6-C₆H₄OMe) ppm.

¹³C NMR (298 K, 125 MHz, Benzene-*d*₆): δ = 55.2 (s, C₆H₄OMe), 115.0 (s, 2,6-C₆H₄OMe), 125.7 (s, 3,5-C₆H₄OMe), 145.6 (s, 1-C₆H₄OMe), 155.8 (s, 4-C₆H₄OMe) ppm.

¹⁵N NMR (298 K, 50 Hz, Benzene-*d*₆): δ = -221.1 (s) ppm.

Elemental analysis. Anal. calc. for C₄₂H₄₂BiN₃O₆ (893.79 g · mol⁻¹): Bi, 23.4; found: Bi, 23.7.

[Bi[N(4-Br-C₆H₄)₂]₃] (1-Br). A solution of bis(4-bromophenyl)amine (998 mg, 3.05 mmol) in THF (8 mL) was cooled to 0 °C and a dispersion of potassium hydride (123 mg, 3.06 mmol) in THF (2 mL) was slowly added. An immediate gas evolution and a color change to slightly yellow were observed. The solution was allowed to warm to ambient temperature while stirring for 2 h. BiI₃ (600 mg, 1.02 mmol) was dissolved in THF (9 mL) and cooled to 0 °C. The yellow amide solution was slowly added with an immediate color change to red. While warming to ambient temperature a white solid precipitated. After stirring for 45 min, all solids were removed by filtration over celite. The solvent was narrowed down to 3 mL under reduced pressure. Pentane (30 mL) was added while stirring leading to precipitation of an orange solid, which was isolated by filtration. The solid was washed with pentane (6 × 5 mL) and dried *in vacuo* for 5 min (exposure to vacuum for extended periods of time leads to decomposition). The product contains n equiv. THF (n needs to be evaluated individually for every batch and typically ranges from 0.3 to 1.0, values given here refer to n = 0.75).

Yield: 1.05 g (0.84 mmol, 83%)

¹H NMR (298 K, 400 MHz, Benzene-*d*₆): δ = 6.15 (d, 12 H, ³J_{HH} = 7.9 Hz, 2,6-C₆H₄Br), 7.13 (d, 12H, ³J_{HH} = 7.9 Hz, 3,5-C₆H₄Br) ppm. Resonances due to THF were also detected.

¹³C NMR (298 K, 126 MHz, Benzene-*d*₆): δ = 116.2 (s, 4-C₆H₄Br), 125.6 (s, 2,6-C₆H₄Br), 132.7 (s, 3,5-C₆H₄Br), 149.3 (s, 1-C₆H₄Br) ppm.

Elemental analysis. Anal. calc. for C₃₆H₃₂BiN₃Br₃ × 0.75 [C₄H₈O] (1187.01 g · mol⁻¹): C, 37.74; H, 2.44; N, 3.39; found: C, 37.38; H, 2.50; N, 3.43.

SUPPORTING INFORMATION

[Bi[N(*p*-biphenyl)₂]₃] (1-Ph). A solution of bis(4,4'-diphenyl)amine (999 mg, 3.11 mmol) in THF (20 mL) was cooled to 0 °C and a dispersion of potassium hydride (125 mg, 3.12 mmol) in THF (2 mL) was slowly added. An immediate gas evolution and a color change to orange were observed. The solution was allowed to warm to ambient temperature while stirring for 4 h. BiI₃ (611 mg, 1.04 mmol) was dissolved in THF (9 mL) and cooled to -78 °C. The amide solution was slowly added with an immediate color change to red. A white solid precipitated. After stirring for 10 min, all solids were removed by filtration over celite. The solvent was removed from the filtrate under reduced pressure. The resulting solid was washed with pentane (6 × 5 mL) and dried *in vacuo* for 5 min (exposure to vacuum for extended periods of time leads to decomposition).

The product contains n equiv. THF (n needs to be evaluated individually for every batch and typically ranges from 0.4 to 1.2, values given here refer to n = 1.0).

Yield: 1.12 g (0.90 mmol, 87%).

¹H NMR (298 K, 500 MHz, Benzene-d₆): δ = 6.99 (d, 12H, ³J_{HH} = 8.0 Hz, 2,12-C₁₂H₉), 7.10 (t, 6H, ³J_{HH} = 7.5 Hz, 8-C₁₂H₉), 7.20 (dd, 12H, ³J_{HH} = 7.5 Hz, ³J_{HH} = 7.4 Hz, 7,9-C₁₂H₉), 7.44 (d, 12H, ³J_{HH} = 6.9 Hz, 6,10-C₁₂H₉) 7.48 (d, 12H, ³J_{HH} = 8.4 Hz, 3,11-C₁₂H₉) ppm. Resonances due to THF were also detected.

¹³C NMR (298 K, 126 MHz, Benzene-d₆): δ = 124.8 (s, 2,12-C₁₂H₉), 127.0 (s, 8-C₁₂H₉), 127.1 (s, 6,10-C₁₂H₉), 128.4 (s, 3,11-C₁₂H₉), 129.1 (s, 7,9-C₁₂H₉), 135.9 (s, 5-C₁₂H₉), 141.1 (s, 4-C₁₂H₉), 150.7 (s, 1-C₁₂H₉) ppm. Resonances due to THF were also detected.

¹⁵N NMR (298 K, 50 Hz, Benzene-d₆): δ = -212.9 (s) ppm.

Elemental analysis. Anal. calc. for C₇₂H₅₄BiN₃ × 1.0 [C₄H₈O] (g · mol⁻¹): C: 73.48; H, 5.03; N, 3.38; found: C, 73.59; H, 4.78; N, 3.43.

[Bi[N(4-CF₃-C₆H₄)₂]₃] (1-CF₃). A solution of bis(4-trifluoromethyl)amine (268 mg, 0.88 mmol) in benzene (2 mL) was added to a solution of tris(dimethylamido)bismuth (**4**) (100 mg, 0.29 mmol) in benzene (2 mL). The reaction mixture was stirred for 5 d at room temperature resulting in a dark red solution. All volatiles were removed under reduced pressure. Washing with pentane (3 × 5 mL) and drying *in vacuo* for 45 min resulted in a violet powder.

Yield: 206 mg (0.18 mmol, 63%).

¹H NMR: (298 K, 400 MHz, Benzene-d₆): δ = 6.30 (d, 12H, ³J_{HH} = 7.85 Hz, 2,6-C₆H₄CF₃), 7.27 (d, 12H, ³J_{HH} = 7.85 Hz, 3,5-C₆H₄CF₃) ppm.

¹⁹F NMR: (298 K, 377 MHz, Benzene-d₆): δ = -61.53 (s) ppm.

¹³C NMR: (298 K, 101 MHz, Benzene-d₆): δ = 123.7 (s, 2,6-C₆H₄CF₃), 124.7 (q, ¹J_{CF} = 271.5 Hz, CF₃), 127.2 (q, ³J_{CF} = 3.6 Hz, 3,5-C₆H₄CF₃), 128.6 (s, 4-C₆H₄CF₃), 152.7 (s, 1-C₆H₄CF₃) ppm.

Elemental analysis. Anal. calc. for C₄₂H₂₄BiF₁₈N₃ (1121.63 g · mol⁻¹): Bi: 18.6; found: Bi: 18.2.

Single Crystal X-ray Analysis

Deposition Numbers 2044877-2044880 contain the supplementary crystallographic information for this work. These data are provided free of charge by the joint Cambridge Crystallographic Data Centre and Fachinformationszentrum Karlsruhe Access Structures service under www.ccdc.cam.ac.uk/structures.

[Bi(NPh₂)₃] (1-H). Analogously to the literature,^[7] **1-H** crystallizes in the triclinic space group P1-H, the margin of error was slightly improved (Bi1–N1: 2.17(2) Å to 2.167(6) Å), however the bonding parameters are in the same order of magnitude.^[7] Weak interactions between the bismuth atom and the phenyl group of a neighboring molecule are present based on distance criteria.

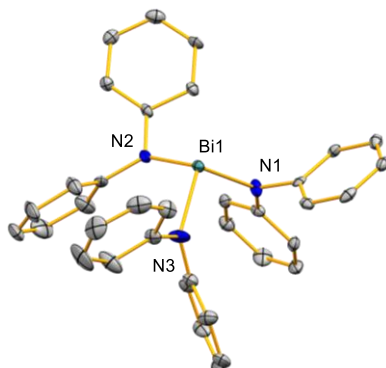


Figure S1. Molecular Structure of **1-H** in the solid state. The elemental cell contains two crystallographically independent, but chemically identical molecules of the bismuth amide. Only one of them is depicted since the bonding parameters are highly similar. Ellipsoids are shown at the 50% probability level; hydrogen atoms are omitted for clarity. Selected bond lengths [Å] and angles[°]: Bi1–N1, 2.167(6); Bi1–N2, 2.184(7); Bi1–N3, 2.148(7); N1–Bi1–N2, 96.8(2); N1–Bi1–N3, 97.0(3); N2–Bi1–N3, 100.3(3); Σ(Bi1) 294, Σ(N1) 360, Σ(N2) 352, Σ(N3) 360.

SUPPORTING INFORMATION

[Bi[N(4-Me-C₆H₄)₂]₃] (1-Me). **1-Me** crystallizes in the triclinic space group $P\bar{1}$ with $Z=2$ (Figure S2a). The bismuth atom is coordinated by three di(*p*-tolyl)amide ligands. The bond angles around Bi1 are $100.68(8)^\circ$ (N1–Bi1–N2), $97.92(8)^\circ$ (N1–Bi1–N3), and 95.03° (N2–Bi1–N3) with an angular sum of 294° around bismuth. This results in a distorted trigonal pyramidal geometry. The two *p*-tolyl substituents of each amide are twisted relatively to each other. The idealized planes defined by the *p*-tolyl groups of each amide ligand form angles of 86.16° (N1), 79.82° (N2), and 59.02° (N3). The distances between Bi1 and the three nitrogen atoms vary between $2.158(2)$ Å (Bi1–N2) and $2.185(2)$ Å (Bi1–N3) which is in accordance with the only literature-known bismuth arylamide **1-H** with distances between $2.149(7)$ Å and $2.183(7)$ Å. The N–Bi–N bond angles are also in the same range as previously reported for **1-H** with angles between $96.7(3)^\circ$ and $100.3(3)^\circ$. The angular sums of the nitrogen atoms are 357° (N1), 359° (N2), and 354° (N3) resulting in a near trigonal planar geometry. The distance between bismuth atoms of neighboring molecules of **1-Me** amounts to 3.79 Å, suggesting Bi···Bi interactions in the solid state (Figure S2b).

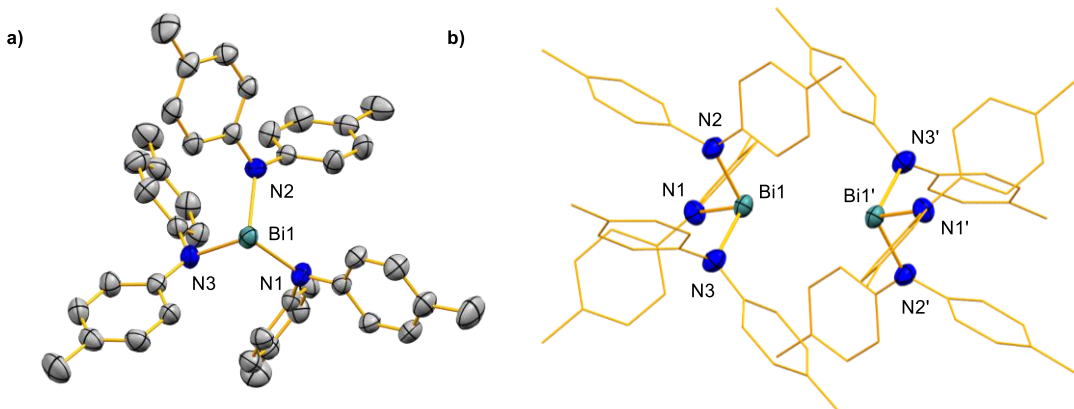


Figure S2. Molecular structure of **1-Me** in the solid state (a: one formula unit; b: two formula unit with potential Bi···Bi interactions). Ellipsoids are set at 50% probability; hydrogen atoms are omitted and carbon atoms in (b) are shown as wireframe for clarity. Selected bond lengths [Å] and angles [°]: Bi1–N1, $2.1598(19)$; Bi1–N2, $2.158(2)$; Bi1–N3, $2.185(2)$; N1–Bi1–N2, $100.68(8)$; N1–Bi1–N3, $97.92(8)$; N2–Bi1–N3, $95.03(8)$; $\Sigma(\text{Bi1})$ 294 , $\Sigma(\text{N1})$ 357 , $\Sigma(\text{N2})$ 359 , $\Sigma(\text{N3})$ 354 .

[Bi[N(4-Br-C₆H₄)₂]₃] (1-Br). **1-Br** crystallizes in the triclinic space group $P\bar{1}$ with $Z=1$ (Figure S3). The bismuth atom Bi1 is coordinated by three bis(*p*-bromophenyl) amide ligands with bond angles of N1–Bi1–N2 $94.18(12)^\circ$, N1–Bi1–N3 $95.03(11)^\circ$ and N2–Bi1–N3 $95.87(11)^\circ$. In comparison to **1-H** and **1-Me**, the three bond angles show less variance with a difference of only 1.69° between the smallest and largest angle (**1-H**: 3.6° ; **1-Me**: 5.7°).^[7] Also, the angular sum of 285° around the bismuth is 9° smaller than observed for the two previously described examples. Nevertheless, this results in a slightly distorted trigonal pyramidal geometry, as well. The two 4-bromophenyl substituents of each amide are twisted relatively to each other. The idealized planes defined by the 4-bromophenyl groups of each amide ligand form angles of 86.03° (N1), 78.39° (N2), and 85.97° (N3). The distances between Bi1 and the three nitrogen atoms vary between $2.157(3)$ Å (Bi1–N2) and $2.172(3)$ Å (Bi1–N1), which is in accordance with $\text{Bi}(\text{NPh}_2)_3$ with distances between $2.149(7)$ Å and $2.183(7)$ Å.^[7] The average Bi–N bond lengths (2.1666 Å) are as long as in **1-Me** (2.1676 Å). The angular sums of the nitrogen atoms are 359° (N1) and 360° (N2, N3), resulting in a trigonal planar geometry. Weak interactions between the bismuth atom and the bromine atom of a neighboring molecule are present based on distance criteria.

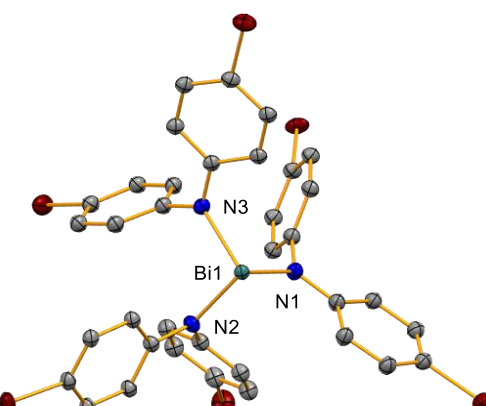


Figure S3. Molecular structure of **1-Br** in the solid state. Ellipsoids are shown at the 50% probability level; hydrogen atoms and two lattice-bound toluene molecules are omitted for clarity. Selected bond lengths [Å] and angles [°]: Bi1–N1 $2.172(3)$, Bi1–N2 $2.157(3)$; Bi1–N3 $2.171(3)$; N1–Bi1–N2 $94.18(12)$, N1–Bi1–N3 $95.03(11)$, N2–Bi1–N3 $95.87(11)$; $\Sigma(\text{Bi1})$ 285 , $\Sigma(\text{N1})$ 359 , $\Sigma(\text{N2})$ 360 , $\Sigma(\text{N3})$ 360 .

SUPPORTING INFORMATION

[Bi[N(4-biphenyl)₂]₃] (1-Ph). **1-Ph** crystallizes in the triclinic space group $P\bar{1}$ with $Z=2$ as a two-component twin (the two domains are related by a rotation around direct lattice direction [100]; Figure S4). The asymmetric unit contains two chemically identical but crystallographically independent molecules, only one of which is discussed due to their similarity. The angular sum around Bi1_{-1} amounts to 303°, resulting in a distorted trigonal pyramidal geometry. The angular sum around the central atom is somewhat larger than that in $\text{Bi}(\text{NPh}_2)_3$ (**1-H**) (294°). The bismuth atom in **1-Ph** is coordinated by three *bis*(4-biphenyl) amide ligands with bond angles between 96.7(2)° (N1_{-1} - Bi1_{-1} - N3_{-1}) and 107.5(3)° (N2_{-1} - Bi1_{-1} - N3_{-1}). The N-Bi-N angles in **1-Ph** span a wider range than those in **1-H** (96.2(3)-100.3(3)).^[7] The greater variance of the bond angles can arise due to π -interactions between the phenyl ring attached to N1_{-1} and the phenyl ring attached to N2_{-1} (3.670 Å). In the ring-slipped π -stacking, the smallest distance of the centroid of one aryl ring to a carbon atom of the other aryl ring (and vice versa) amounts to 3.32 Å (and to 3.59 Å), suggesting a significant interaction.^[8] The high steric demand of the *bis*(4-biphenyl) amide substituents may also contribute to the N-Bi-N bond angles differing from those in **1-H**, **1-Me**, and **1-Br**. In addition, the Bi-N bonds in **1-Ph** (2.16-2.23 Å) are slightly elongated compared to those in **1-H** (2.15-2.18 Å), **1-Me** (2.16-2.19 Å), and **1-Br** (2.16-2.17 Å). Weak interactions between the bismuth atom and the phenyl group of a neighboring molecule are present based on distance criteria.

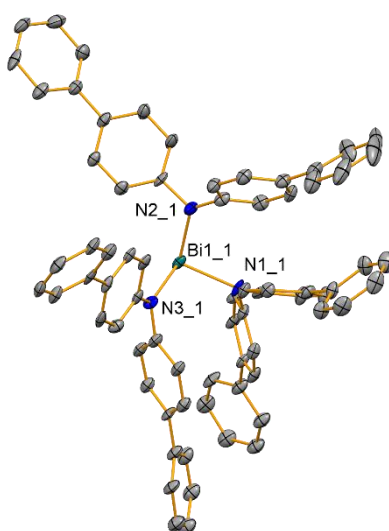


Figure S4. Molecular structure of **1-Ph** in the solid state. The elemental cell contains two crystallographically independent, but chemically identical molecules of the bismuth amide. Only one of them is depicted since the bonding parameters are highly similar. Ellipsoids are shown at the 50% probability level; hydrogen atoms and one lattice-bound THF molecule are omitted for clarity. Selected bond lengths [Å] and angles [°]: Bi1_{-1} - N1_{-1} 2.197(6), Bi1_{-1} - N2_{-1} 2.162(7), Bi1_{-1} - N3_{-1} 2.230(6); N1_{-1} - Bi1_{-1} - N2_{-1} 98.4(3), N2_{-1} - Bi1_{-1} - N3_{-1} 107.5(2), N1_{-1} - Bi1_{-1} - N3_{-1} 96.7(2); $\Sigma(\text{Bi1}_{-1})$ 303, $\Sigma(\text{N1}_{-1})$ 360, $\Sigma(\text{N2}_{-1})$ 360, $\Sigma(\text{N3}_{-1})$ 359.

Literature-Known Bismuth Amides and Related Species

A small group of bismuth compounds with amide ligands that contain one aryl group, $(\text{NArR})^-$, has been reported ($\text{R} = \text{H, Si(alkyl)}_3$). These include mono-, di-, and trinuclear complexes of type $[\text{Bi}(\text{NArR})_3]$, $[\text{BiZ}_2(\text{NArR})]$, $[\text{Bi}_2(\text{NAr})_2(\text{NHAr})_2]$, and $[\text{Bi}_3(\text{NAr})_4(\text{NHAr})]$ ($\text{Z} = \text{halide, weakly coordinating anion}$).^[9]

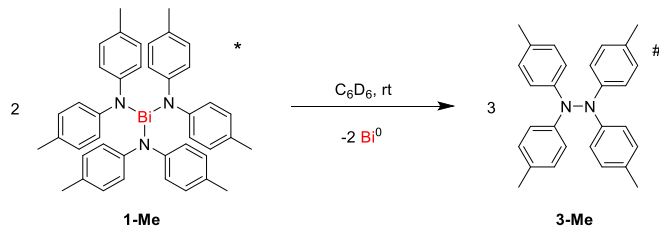
Unforeseen reactions such as CH activation,^[9a, 9f] dearomatization,^[9f] N-Si bond cleavage,^[10] Bi-N/B-Li metathesis,^[9d] methyl migration (from Si to Bi),^[9g] and transamination/aggregation sequences^[9j] have been documented for these species, but have not mechanistically been rationalized in many cases.

As outlined in the main part, homolytic Bi-O bond cleavage has previously been discussed in the context of the SOHIO process.^[11] Different mechanistic scenarios have also been discussed in the SOHIO process and have recently been suggested to be more likely based on kinetic investigations.^[12]

SUPPORTING INFORMATION

Reaction Monitoring: Formation of Compounds 3-X from 1-X

General procedure: a sample of the bismuth compound (**1-H**, **1-Me**, **1-OMe**, **1-Br**, or **1-Ph**, respectively; $n = 1.25 \cdot 10^{-5}$ mmol in each case) was dissolved in C_6D_6 (0.5 mL) at room temperature and the progress of the reaction was monitored by 1H NMR spectroscopy. Examples of the reaction equation and selected NMR spectra are shown in Scheme S1 and Figure S5 for compound **1-Me**. Half-life periods were determined (Table S1).



Scheme S1. Formation of **3-Me** from **1-Me** in an N–N bond formation reaction.

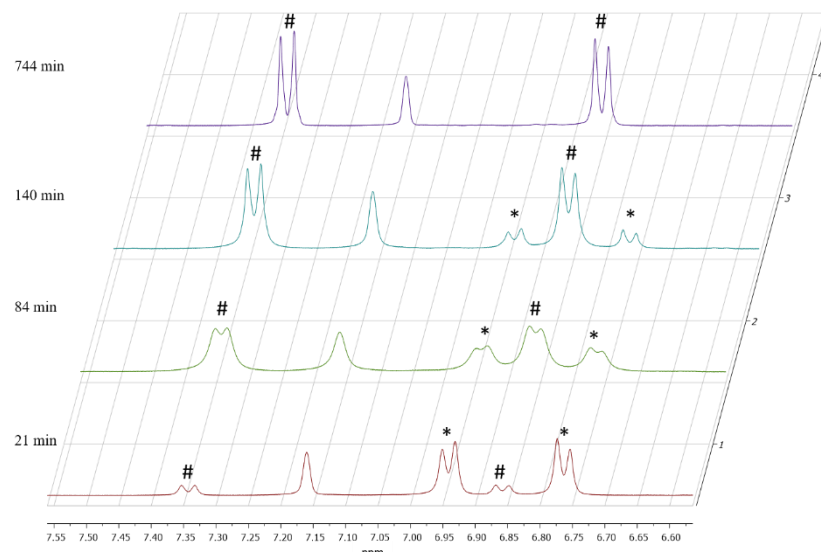


Figure S5. Aromatic region of the 1H NMR spectra of **1-Me** over time. The intensity of the doublets of the bismuth amide at 6.77 (*) and 6.95 (*) ppm decreases whereas the intensity of the doublets of the hydrazine derivative **3-Me** at 6.87 (#) and 7.35 (#) ppm increases over time.

Table S1. Half-life periods of the bismuth amides **1-X** in their selective N–N bond formation reactions in benzene at 23 °C.

Compound	$t_{1/2}$ [h]	Compound	$t_{1/2}$ [h]
1-H	63	1-Me	1.4
1-OMe	1.2	1-Br	84
1-Ph	74	1-CF₃	stable

SUPPORTING INFORMATION

Kinetic Investigations of Formation of 3-Me from 1-Me

General procedure: 5 mg ($6.2 \cdot 10^{-3}$ mmol), 10 mg ($1.3 \cdot 10^{-2}$ mmol), 15 mg ($1.9 \cdot 10^{-2}$ mmol), 30 mg ($3.7 \cdot 10^{-2}$ mmol), or 45 mg ($5.6 \cdot 10^{-2}$ mmol) of **1-Me** were dissolved in C₆D₆ (0.5 mL) and the progress of the formation of **3-Me** was monitored by ¹H NMR spectroscopy at 23 °C and determined by the integration intensity of the ¹H NMR spectroscopic resonances of the methyl groups of **1-Me** and **3-Me**. The related time-conversion plot is shown in Figure S6. It is apparent that higher initial concentrations of **1-Me** decrease the rate at which **3-Me** is formed. In agreement with this, the aggregation of two equivalents **1-Me** to give the dinuclear species (**1-Me**)₂ was found to be exothermic ($\Delta H = -29.6$ kcal·mol⁻¹) and exergonic ($\Delta G = -6.6$ kcal·mol⁻¹) according to DFT calculations. Analyses of kinetic parameters of the reaction are hampered by the fact that at least three (and probably more) elementary steps are involved in the reaction and that no intermediates could be detected or isolated (in agreement with the energies of potential intermediates investigated by DFT calculations). Visual kinetic analyses^[13] suggest that the *apparent* order of the reaction in **1-Me** amounts to 0.5 at low initial concentrations of **1-Me** ($C_{\text{low}} \leq 25$ mmol·L⁻¹ (up to 10 mg of **1-Me** under our conditions)), but deviates from this value at higher initial concentrations (Figure S7). Thus, the kinetic analyses confirm the complexity and suggest a concentration-dependency of the reaction mechanism.

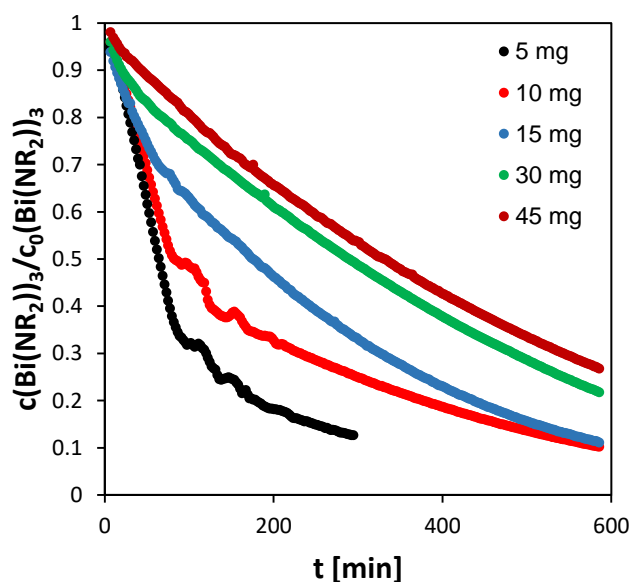


Figure S6. Concentration-dependency of the formation of **3-Me** from **1-Me**.

SUPPORTING INFORMATION

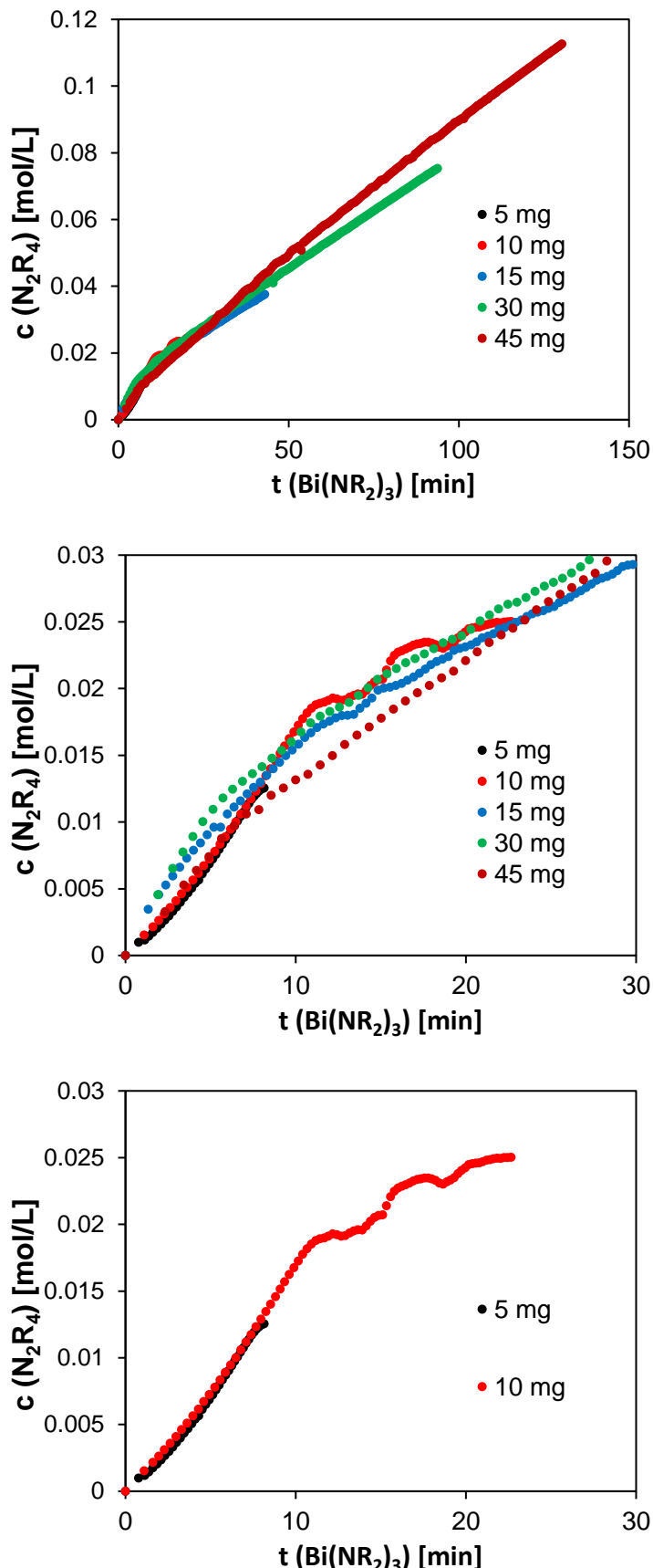


Figure S7. Plots according to Variable Time Normalisation Analysis (VTNA) for **1-Me** (i.e. R = 4-Me-C₆H₄).^[13] Plots show the result obtained for a reaction order of 0.5. Variation of this parameter did not result in a better fit of all data. The graphs show plots of all initial concentrations (top), all initial concentrations in a selected region (middle), and the lowest concentrations (bottom).

SUPPORTING INFORMATION

NMR Spectroscopic data of the hydrazine derivatives 3-X

Reaction of **1-H** yielding **3-H**:

¹H NMR: (298 K, 400 MHz, Benzene-*d*₆): δ = 6.71 (t, 4H, ³J_{HH} = 7.2 Hz, 4-C₆H₅), 6.99 (dd, 8H, ³J_{HH} = 7.8 Hz, 3,5-C₆H₅), 7.32 (d, 8H, ³J_{HH} = 7.9 Hz, 2,6-C₆H₅) ppm.

¹H NMR: (298 K, 400 MHz, Chloroform-*d*₁): δ = 6.90 (t, 4H, 4-C₆H₅), 7.21 (dd, 8H, 3,5-C₆H₅), 7.32 (d, 8H, 2,6-C₆H₅) ppm.^[14]

¹³C NMR: (298 K, 125 MHz, Methylenechloride-*d*₂): δ = 118.6 (s, 2,6-C₆H₅), 122.7 (s, 4-C₆H₅), 129.9 (s, 3,5-C₆H₅), 143.0 (s, 1-C₆H₅) ppm.

The ¹³C NMR spectroscopic data of **3-H** furthermore provides an explanation of the reported ¹³C NMR spectroscopic data of **1-H** (*vide supra*). Closer investigation of the literature known compound **1-H** showed the expected four signals in the aromatic region of the ¹³C NMR spectrum for the phenyl groups (**1-H**: 122.5, 124.5, 129.6, 151.3 ppm (in C₆D₆)). This is in contrast to the NMR spectroscopic data reported, which shows seven resonances in the aromatic region, however in dichloromethane (DCM).^[7] We found that four of these signals can be assigned to **1-H** and the other three to Ph₄N₄ (**3-H**). The resonance at 122.7 ppm (in DCM) represents two overlapping signals (4-C₆H₅ of **1-H** and 4-C₆H₅ of **3-H**).

Reaction of **1-Me** yielding **3-Me**:

¹H NMR (298 K, 400 MHz, Benzene-*d*₆): δ = 2.01 (s, 12H, C₆H₄Me), 6.86 (d, 8H, ³J_{HH} = 8.3 Hz, 2,6-C₆H₄Me), 7.34 (d, 8H, ³J_{HH} = 8.4 Hz, 3,5-C₆H₄Me) ppm.

¹H NMR (298 K, 400 MHz, Chloroform-*d*₁): δ = 2.23 (s, 12H, C₆H₄Me), 6.98 (d, 8H, ³J_{HH} = 8.4 Hz, 2,6-C₆H₄Me), 7.17 (d, 8H, ³J_{HH} = 8.6 Hz, 3,5-C₆H₄Me) ppm.^[14]

¹³C NMR (298 K, 125 MHz, Benzene-*d*₆): δ = 20.6 (s, C₆H₄Me), 118.5 (s, 2,6-C₆H₄Me), 130.1 (s, 3,5-C₆H₄Me), 131.2 (s, 4-C₆H₄Me), 142.0 (s, 1-C₆H₄Me) ppm.

Reaction of **1-OMe** yielding **3-OMe**:

¹H NMR (298 K, 400 MHz, Benzene-*d*₆): δ = 3.27 (s, 12H, C₆H₄OMe), 6.70 (d, 8H, ³J_{HH} = 9.0 Hz, 2,6-C₆H₄OMe), 7.31 (d, 8H, ³J_{HH} = 9.0 Hz, 3,5-C₆H₄OMe) ppm.

Identification also by EPR spectroscopy (*vide supra*).

Reaction of **1-Br** yielding in **3-Br**:

¹H NMR (298 K, 400 MHz, Benzene-*d*₆): δ = 6.63 (d, 8H, ³J_{HH} = 9.0 Hz, 2,6-C₆H₄Br), 7.07 (d, 8H, ³J_{HH} = 9.0 Hz, 3,5-C₆H₄Br) ppm.

¹H NMR (298 K, 400 MHz, Chloroform-*d*₁): δ = 7.34 (d, J = 8.8 Hz, 8H), 7.10 (d, J = 8.8 Hz, 8H)^[14]

Reaction of **1-Ph** yielding in **3-Ph**:

¹H NMR (298 K, 400 MHz, Benzene-*d*₆): δ = 7.10 (t, 4H, 8-C₁₂H₉, ³J_{HH} = 7.5 Hz), 7.19 (dd, 8H, ³J_{HH} = 7.7 Hz, 7,9-C₁₂H₉), 7.42 (m, 16H, 2,6,10,12-C₁₂H₉), 7.51 (d, 8H, ³J_{HH} = 8.5 Hz, 3,11-C₁₂H₉) ppm.

Reaction of 1-Me and 1-Br in C₆D₆

Mixing of **1-Me** and **1-Br** in a 1:1 ratio in C₆D₆ resulted in the formation of **3-Me**, **3-Br** and the hetero-coupled product, (4-Me-C₆H₄)₂N-(4-Br-C₆H₄)₂, in a statistically expected ratio of 1:1:2 after 5 days. This suggests rapid ligand exchange between **1-Me** and **1-Br**, which was verified by instantaneous NMR-spectroscopic analysis of the above-mentioned reaction mixture.

1-Br (15.5 mg, 1.25·10⁻² mmol) and **1-Me** (10.0 mg, 1.25·10⁻² mmol) were dissolved in C₆D₆ (0.5 mL) and the reaction monitored by ¹H NMR spectroscopy. In the first spectrum, measured after 10 min, neither **1-Br** nor **1-Me** were identified indicating rapid ligand exchange. A black solid precipitated. After 7 days, a colorless solution had formed and ¹H NMR spectroscopy allowed the identification of **3-Me**, **3-Br** and **3-Br/Me** (cross-coupled hydrazine derivative) by comparison to previous recorded spectra in a statistical distribution of 1:1:2. The products were confirmed by mass spectrometry.

HR-ASAP-MS, positive mode, found: m/z = 648.8120; calculated for C₂₄H₁₇Br₄N₂⁺: m/z = 648.8125; m/z = 521.0223; calculated for C₂₆H₂₃Br₂N₂⁺: m/z = 521.0228; m/z = 393.2236; calculated for C₂₈H₂₉N₂⁺: m/z = 393.2331.

SUPPORTING INFORMATION

Reactivity of secondary pnictogens towards bismuth amides

A defined amount of the required bismuth amide (typically 0.1–0.3 mmol) was dissolved in C₆D₆ at room temperature in a silanized J. Young-type NMR tube, and the required amount of a secondary pnictogen was added (typically 0.1–0.3 mmol). The ratios (n[(Bi(NR₂)₃)]/m(HER'₂) (E = N, P, As) are given in Table S2. However, as initial ratio 1:3 was chosen. If required, further equivalents of the bismuth amide were added resulting in the ratios described in Table S2. If this was required, the reactions were repeated with the final ratios with same results. The reaction mixture was kept at the desired temperature (23 °C or 60 °C, see Table S2). The formation of a side product was obtained in some cases (entries 3, 5, 6, 9), which was identified as product of the P–N bond formation in the case of entry 2^[15]. In order to obtain the correct spectroscopic yield, traces of PCy₃ were added as internal standard to each reaction (one spectrum of the phosphane with PCy₃ was recorded and then the required amount of the bismuth amide was added and additional spectra were recorded). The experiments were also performed in the absence of PCy₃ and no relevant difference was observed. Furthermore, quantitative ³¹P NMR spectra of selected reactions were recorded to exclude integration errors.

Entries 18–21 show that no reactions were observed between bulky dialkylphosphanes and **1-Me**, while **4** reacted with these phosphanes. This highlights the different reactivity of aryl-substituted amides in comparison to alkyl-substituted amides. However, for HAsPh₂ as a substrate, no difference in reactivity between **4** and **1-Me** was observed, and the same yields of the coupled product were obtained (see entries 22 and 23).

Analytical data for P₂Xyl₄. Compound P₂Xyl₄ (*cf.* Table S2, entries 11,12) has previously been synthesized,^[16] but analytical data were not reported in detail. From reactions performed under the conditions described in Table S2 (entry 12), the following analytical data were obtained for P₂Xyl₄: ¹H NMR (298 K, 400 MHz, benzene-d₆): δ = 1.99 (s, 24H, C₆H₃Me₂), 6.69 (s, 4H, 4-C₆H₃Me₂), 7.40 (s, 8H, 2,6-C₆H₃Me₂) ppm; for ³¹P NMR data see Table S2; HR-LIFDI-MS, positive mode, found: m/z = 482.2280; calculated for [P₂Xyl₄]^{•+}: m/z = 482.2287; m/z = 241.1136; calculated for [PXyl₂]^{•+}: m/z = 241.1141.

Table S2. Summary of reaction conditions and yields of the dehydrocoupling reaction.

		Bi(NR ₂) ₃	+ 3 HER' ₂	→	Bi ⁰	+ 3 HNR ₂	+ 1.5 R' ₂ E—ER' ₂		
#	Reagent	Substrate	Conditions		Ratio (n(Reagent)/n(Substrate))	Yield ^[a] [%]	³¹ P NMR C ₆ D ₆ (ppm)	³¹ P NMR CDCl ₃ (ppm)	³¹ P NMR CD ₂ Cl ₂ (ppm)
1	4	HN(ptol) ₂	rt, 3 d		1:3	85	/	/	/
2	4	HPPh ₂	rt, t < 7 min		1:3	80 ^[b]	-14.8 ^[4]	/	/
3	1-Me	HPPh ₂	rt, t < 7 min		1:3	Quant.	-14.8 ^[4]	/	/
4	4	HP(4-Cl-Ph) ₂	rt, t < 7 min		2:3	78 ^[b]	-17.3	/	-17.7 ^[4]
5	1-Me	HP(4-Cl-Ph) ₂	rt, t < 3 h		1.2:3	97	-17.3	/	-17.7 ^[4]
6	4	HP(4-OMe-Ph) ₂	rt, t < 7 min		1:3	65 ^[b]	-18.9	/	-20.1 ^[4]
7	1-Me	HP(4-OMe-Ph) ₂	rt, t < 2 h		1.5:3	92 ^[b]	-18.9	/	-20.1 ^[4]
8	4	HP(4-CF ₃ -Ph) ₂	rt, t < 15 min		2:3	77 ^[b]	-14.3 ^[3]	/	/
9	1-Me	HP(4-CF ₃ -Ph) ₂	rt, t < 3 h		2:3	Quant.	-14.3 ^[3]	/	/
10	4	HPMes ₂	rt, 16 h		2:3	Quant.	-30.4	-30.0 ^[16]	/
11	4	HP(Xyl) ₂ ^[c]	rt, 15 min		2:3	80 ^[b]	-15.6	/	/
12	1-Me	HP(Xyl) ₂ ^[c]	rt, 3 h		2:3	90 ^[b]	-15.6	-14.8	/
13	4	HP <i>i</i> Pr ₂	rt, t < 3.5 h		1.2:3	96 ^[b]	-12.1 ^[17]	/	/
14	1-Me	HP <i>i</i> Pr ₂	rt, t < 6 h		1.2:3	99 ^[b]	-12.1 ^[17]	/	/
15	4	HP(C ₅ H ₉) ₂ ^[d]	rt, t < 3 h		2:3	94 ^[b]	-10.8 ^[18]	/	/
16	1-Me	HPCy ₂	rt, 1.5 h		1:3	Quant.	-21.7 ^[19]	-21.4	/
17	4	HPCy ₂	rt, 6 h		1:3	85 ^[b]	-21.7 ^[19]	-21.4	/
18	4	HP <i>t</i> Bu ₂	60 °C, 1 d		2:3	Quant.	-39.8 ^[20]	-41.3 ^[21]	/
19	1-Me	HP <i>t</i> Bu ₂	rt, 6 d		1:3	n.d.			
20	4	HPAd ₂ ^[e]	60 °C, 2 d		2:1	Quant.	33.2	34.3 ^[22]	/
21	1-Me	HPAd ₂ ^[e]	60 °C, 4 h		1:3	n.d.	/	/	/
22	4	HAsPh ₂	-78 °C, t < 7 min		1:3	80 ^{[b][f]}	/	/	/
23	1-Me	HAsPh ₂	rt, t < 7 min		1:3	80 ^{[b][f]}	/	/	/

[a] determined by ¹H and/or ³¹P NMR spectroscopy. [b] lower yield due to E–N bond formation. [c] Xyl = 3,5-Me₂-C₆H₃. [d] = cyclopentyl. [e] Ad = adamantyl. [f] identification by comparison of ¹H NMR spectroscopic data;^[23] quant. = quantitative; n.d. = not detected.

SUPPORTING INFORMATION

Reactions of bismuth amides such as **1-Me** and **4** with phosphanes to give diphosphanes involve at least two types of elementary reactions. These are i) the formation of a species with a Bi–P bond and ii) the homolysis of Bi–P bonds to release phosphorus-centered radicals as discussed in the main text and shown through EPR-spectroscopic experiments.

The following observations are helpful for a discussion of the first step of these reactions (Bi–P bond formation): Reactions of **1-Me**, **1-H**, and **4** with 3 equiv. HPPH₂ all gave **5-Ph** as the main product in instantaneous reactions. Reactions of **4** with HPAd₂ gave **5-Ad**, while reaction of **1-Me** with HPAd₂ mainly gave **3-Me** (and unreacted HPAd₂). These observations demonstrate that the formation of the P–P coupling products does not correlate with the ability of the bismuth amide precursors to form aminyl radicals. We thus propose that the initiating step of the reaction (the reaction of a Bi–NR₂ functional group with HPR'₂ to give a Bi–PR₂ functional group and HNR₂) may well proceed in a polar fashion.

Work-up protocol for the isolation of diphosphanes. Work-up protocols for the isolation of diphosphanes are presented, using the coupling reaction of *t*Bu₂PH with **4** and (4-Cl-Ph)₂PH with **1-Me** as examples. These protocols were optimized for simplicity of the work-up procedure rather than maximized isolated yield.

In a silanized J. Young-type NMR tube, *t*Bu₂PH (13 mg, 0.089 mmol) was dissolved in 0.5 mL C₆D₆. **4** (20 mg, 0.059 mmol) was added and the reaction mixture was kept at 60 °C for one day. After completion of the reaction, the black precipitate was removed by filtration, and all volatiles (solvent and the by-product dimethylamine) were removed under reduced pressure. The product was isolated as white powder.

Yield: 10.4 mg (0.036 mmol, 81%).

This simple work up procedure should be suitable for the alkyl substituted diphosphanes.

¹H NMR (298 K, 400 MHz, Chloroform-*d*₁): δ = 1.38 (t, 36H, ³J_{PH} = 6.2 Hz, CH₃) ppm.^[21]

³¹P NMR (298 K, 162 MHz, Chloroform-*d*₁): δ = -41.3 (s) ppm.^[21]

In a silanized flask, (4-Cl-Ph)₂PH (60 mg, 0.235 mmol) was dissolved in benzene (3 mL) and a solution of **1-Me** (75 mg, 0.094 mmol) in benzene (2 mL) was added. The reaction mixture was stirred at room temperature for 16 h until a slightly yellow color of the liquid phase and a black precipitate were observed. The black solid was removed by filtration, and all volatiles were removed under reduced pressure. The white residue was washed with pentane (5 × 2 mL). The product was isolated as white powder.

Yield: 45 mg (0.089 mmol, 76%).

¹H NMR (298 K, 400 MHz, Methylenechloride-*d*₂): δ = 7.22 – 7.25 (m, 8H, 3,5-C₆H₄Cl), 7.28 – 7.31 (m, 8H, 2,6-C₆H₄Cl) ppm.

³¹P NMR (298 K, 162 MHz, Methylenechloride-*d*₂): δ = -17.7 (s) ppm.^[4]

Comparison with literature protocols. In the main part, the results on phosphane dehydrocoupling presented in this work have been compared to literature-known protocols that are based on main group species in some detail. A more detailed comparison with protocols that are based on transition metal compounds is presented here. It has to be noted that catalytic reactions are possible with transition metal species based on elements such as titanium, zirconium, iron, and rhodium.^[3, 18, 24] However, long reaction times from ca. 8 hours and up to 12 days were required, even for substrates such as HPPH₂.^[3, 18, 24c, 24d, 24f] In addition, elevated temperatures (typically 70–140°C) were applied for efficient conversion of the same substrate.^[3, 18, 24c, 24d, 24f] In comparison, the stoichiometric reaction of **1-Me** with HPPH₂ proceeds at room temperature (or below) to give Ph₂P–PPH₂ in quantitative amounts in less than 10 minutes. Most importantly, the substrate scope includes dialkylphosphanes with moderate steric bulk (e.g. HP(cyclohexyl)₂) as well as very bulky dialkyl and diarylphosphanes such as HP(adamantyl)₂ and HP(mesityl)₂, when bismuth species are applied. In contrast, the conversion of bulky dialkyl or diaryl phosphanes was generally more problematic in the case of transition metal catalysis^[3, 18, 24] (for instance: HPtBu₂ showed no conversion with a rhodium catalyst),^[18] in some cases dialkylphosphanes with moderate (HP(cyclohexyl)₂)^[18] or low steric profiles (HPEt₂)^[24c] showed low conversions, and in some cases of transition metal catalysis only the conversion of primary phosphanes has been reported.^[24e]

SUPPORTING INFORMATION

EPR Spectroscopic Measurements

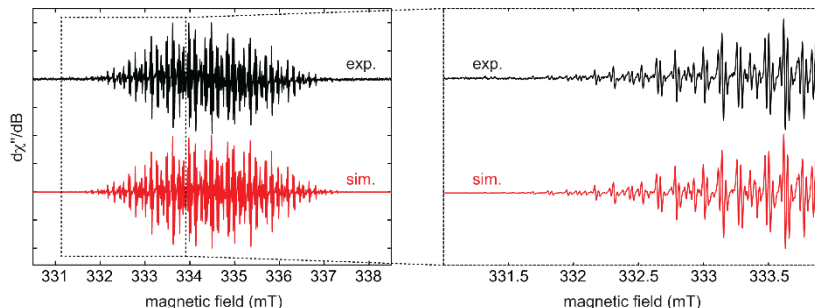


Figure S8. Experimental (black) and simulated (red) continuous-wave (CW) X-band EPR spectra of the degradation of **1-Me** in benzene. The spectra are in accordance with reported data of the di(*p*-tolyl)aminyl radical.^[25] The observed resonance shows coupling constants of $a(^{14}N) = 24.3$ MHz (8.7 G), $a(^1H) = 13.3$, 10.1, 4.0 MHz (4.8, 3.6, 1.4 G) and a g_{iso} value of 2.0036. Spectrometer settings: microwave frequency = 9.38 GHz, 0.1 G modulation amplitude at 100 kHz, power = 0.2 mW, number of accumulated scans = 29, conversion time = 40 ms.

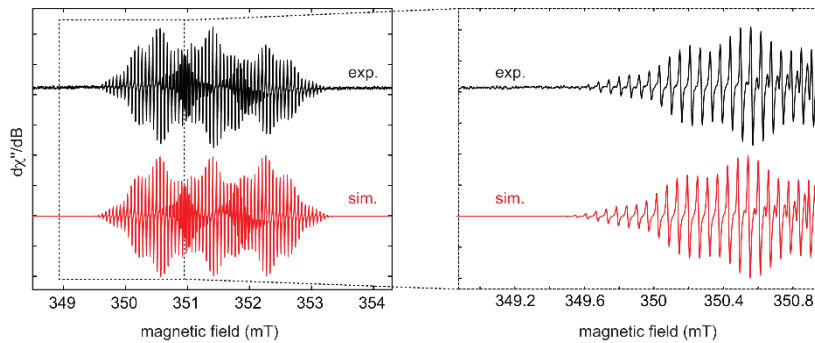


Figure S9. Experimental (black) and simulated (red) continuous-wave (CW) X-band EPR spectra of the degradation **1-OMe** in benzene. The spectra are in accordance with reported data of the di(*p*-methoxyphenyl)aminyl radical.^[25] The observed resonance shows coupling constants of $a(^{14}N) = 23.9$ MHz (8.7 G), $a(^1H) = 9.8$, 3.3, 1.7 MHz (3.5, 1.2, 0.6 G) and a g_{iso} value of 2.0037. Spectrometer settings: microwave frequency = 9.86 GHz, 0.1 G modulation amplitude at 100 kHz, power = 0.2 mW, number of accumulated scans = 19, conversion time = 40 ms.

The observed spectrum has its origin in the homolytic Bi–N bond cleavage (as observed for **1-Me**) and the dissociation of **3-OMe**.^[25]

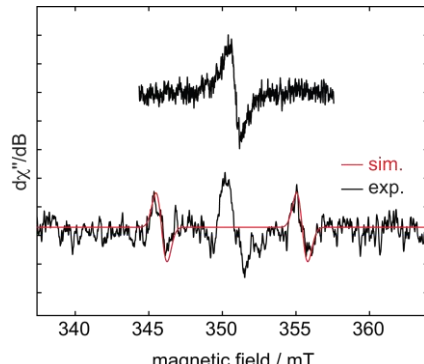


Figure S10. Experimental (black) and simulated (red) continuous-wave (CW) X-band EPR spectra of **4** (top) and of the reaction of **4** with Mes₂PH (bottom) in benzene. The observed doublet has an isotropic coupling constant of $a(^{31}P) = 270$ MHz (96 G) and a g_{iso} value of 2.007. Spectrometer settings: microwave frequency = 9.85 GHz, 1 G modulation amplitude at 100 kHz, power = 4 mW, number of accumulated scans = 48, conversion time = 20 ms. The resonance detected in solutions of **4** could not be removed by sublimation of the bismuth amide.

SUPPORTING INFORMATION

NMR Spectra of Isolated Compounds

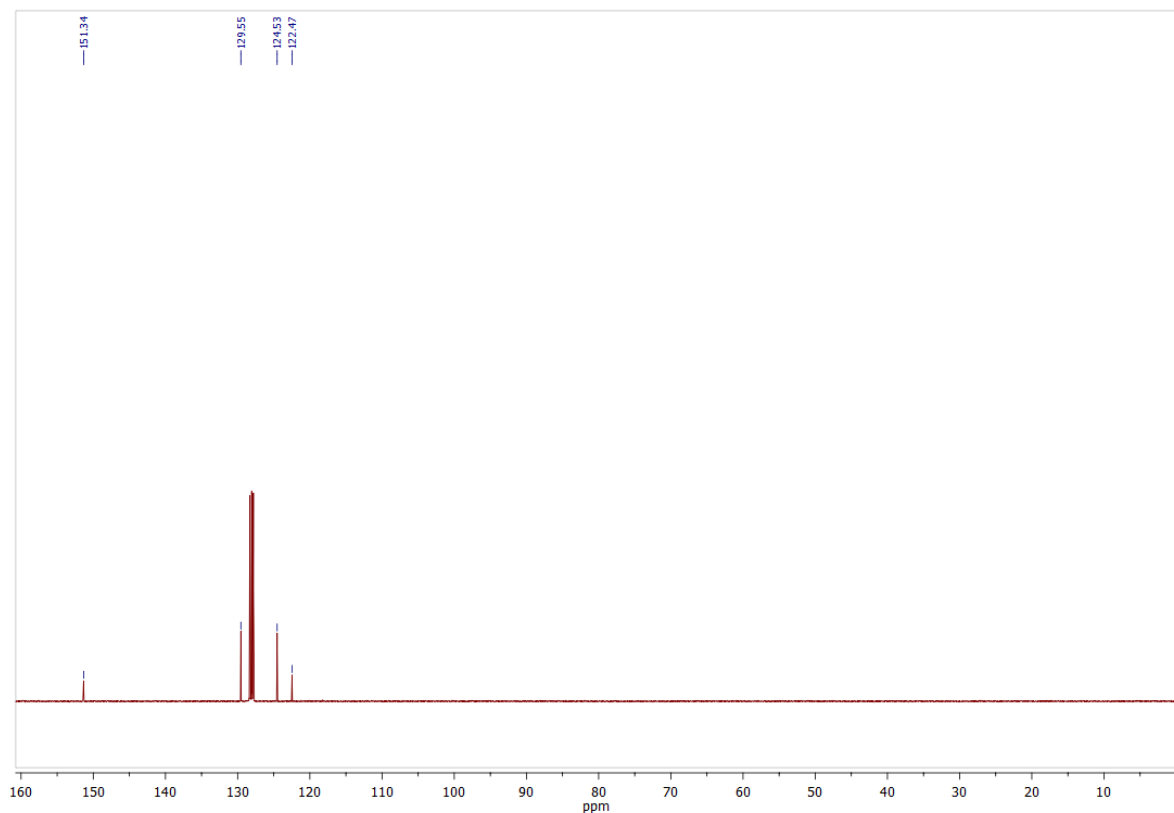
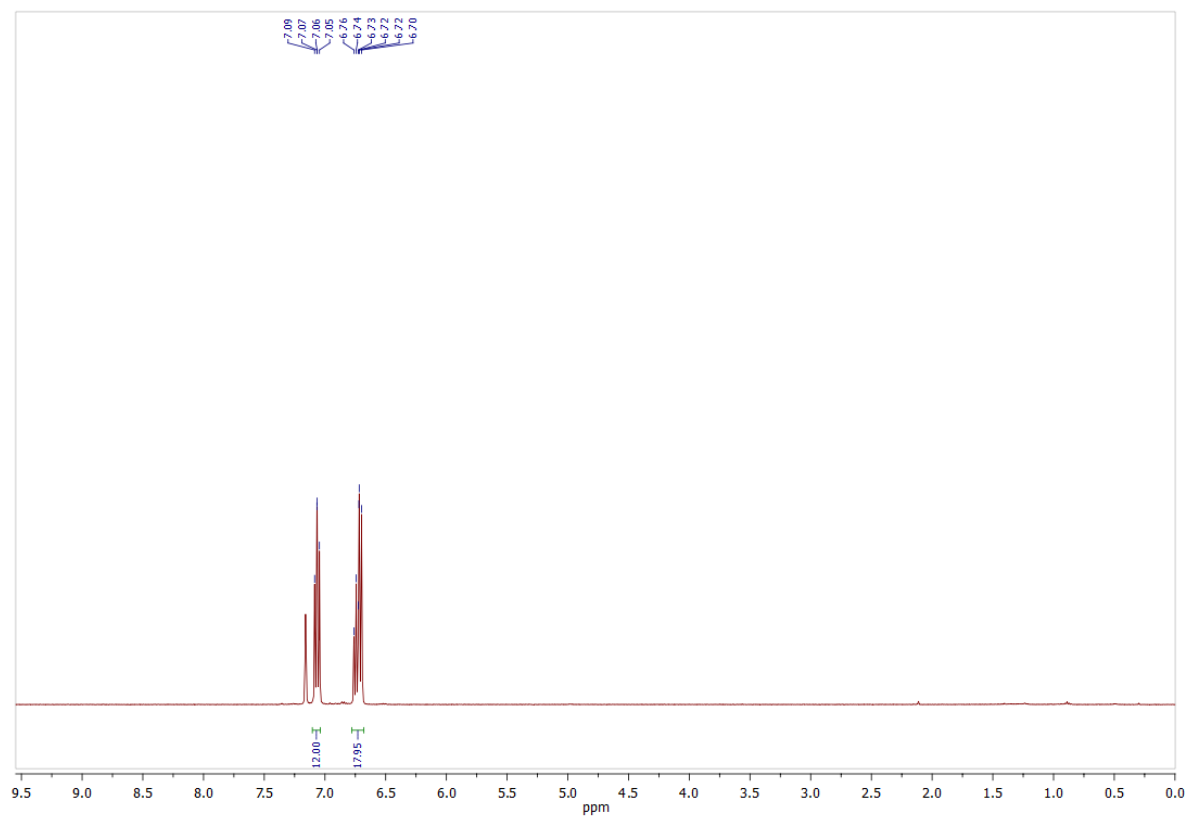


Figure S11. ^1H and ^{13}C spectra of $[\text{Bi}(\text{NPh}_2)_3]$ (1-H) in $\text{Benzene}-d_6$.

SUPPORTING INFORMATION

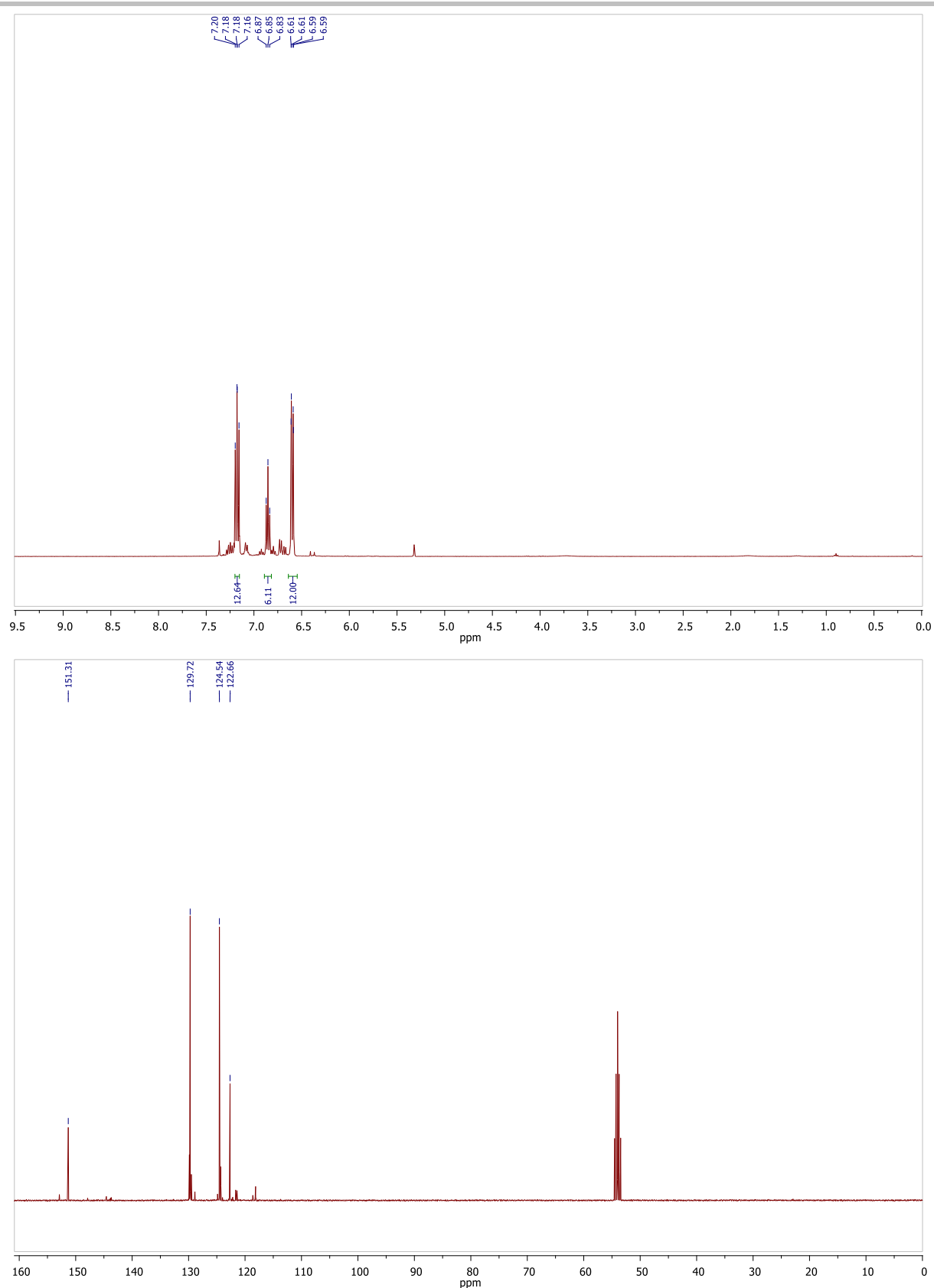


Figure S12. ^1H and ^{13}C spectra of $[Bi(NPh_2)_3]$ (1-H) in Methylenedichloride- d_2 . Decomposition due to the choice of solvent can be observed in both spectra.

SUPPORTING INFORMATION

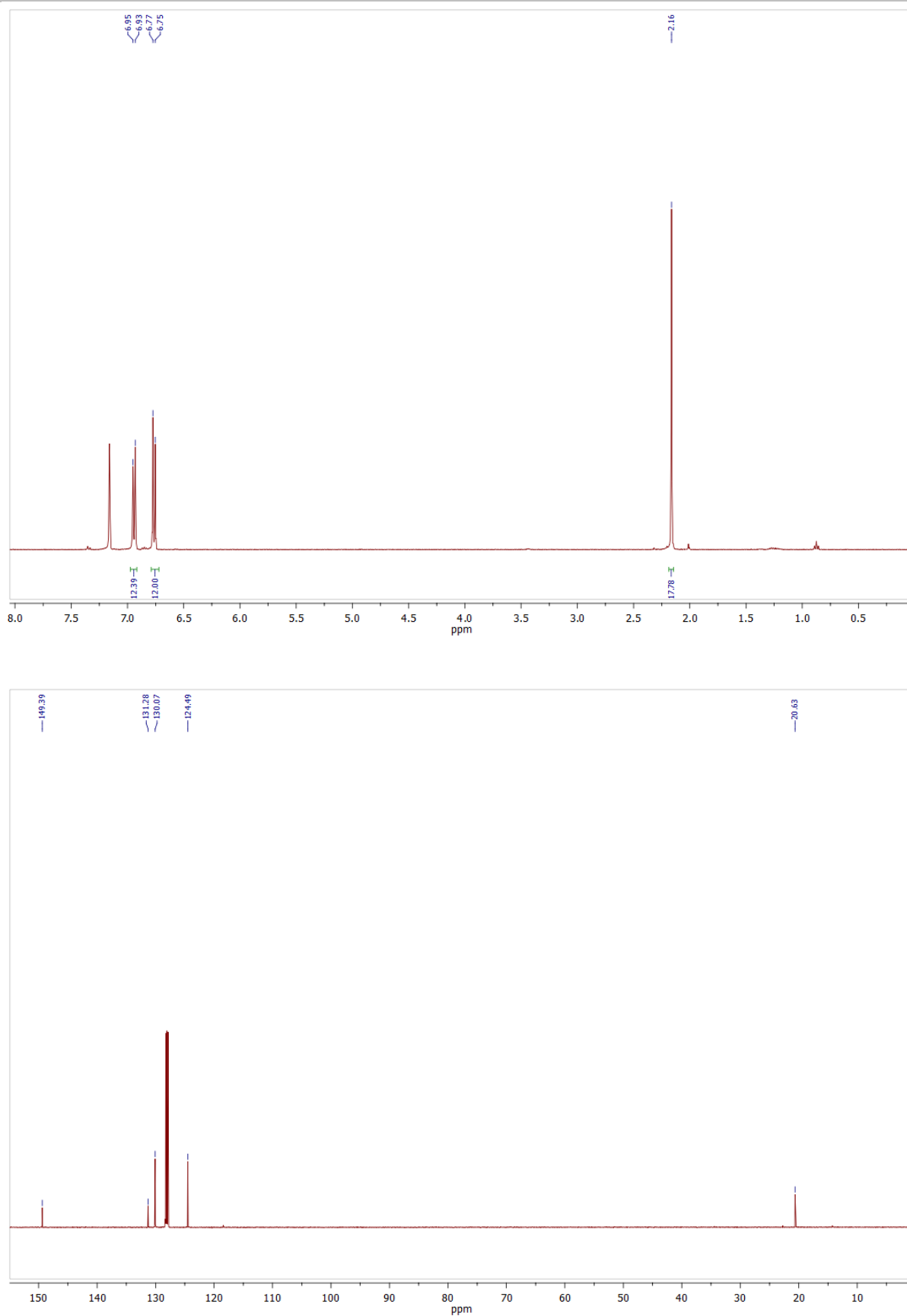


Figure S13. ^1H and ^{13}C spectra of compound **1-Me** in $\text{Benzene}-d_6$.

SUPPORTING INFORMATION

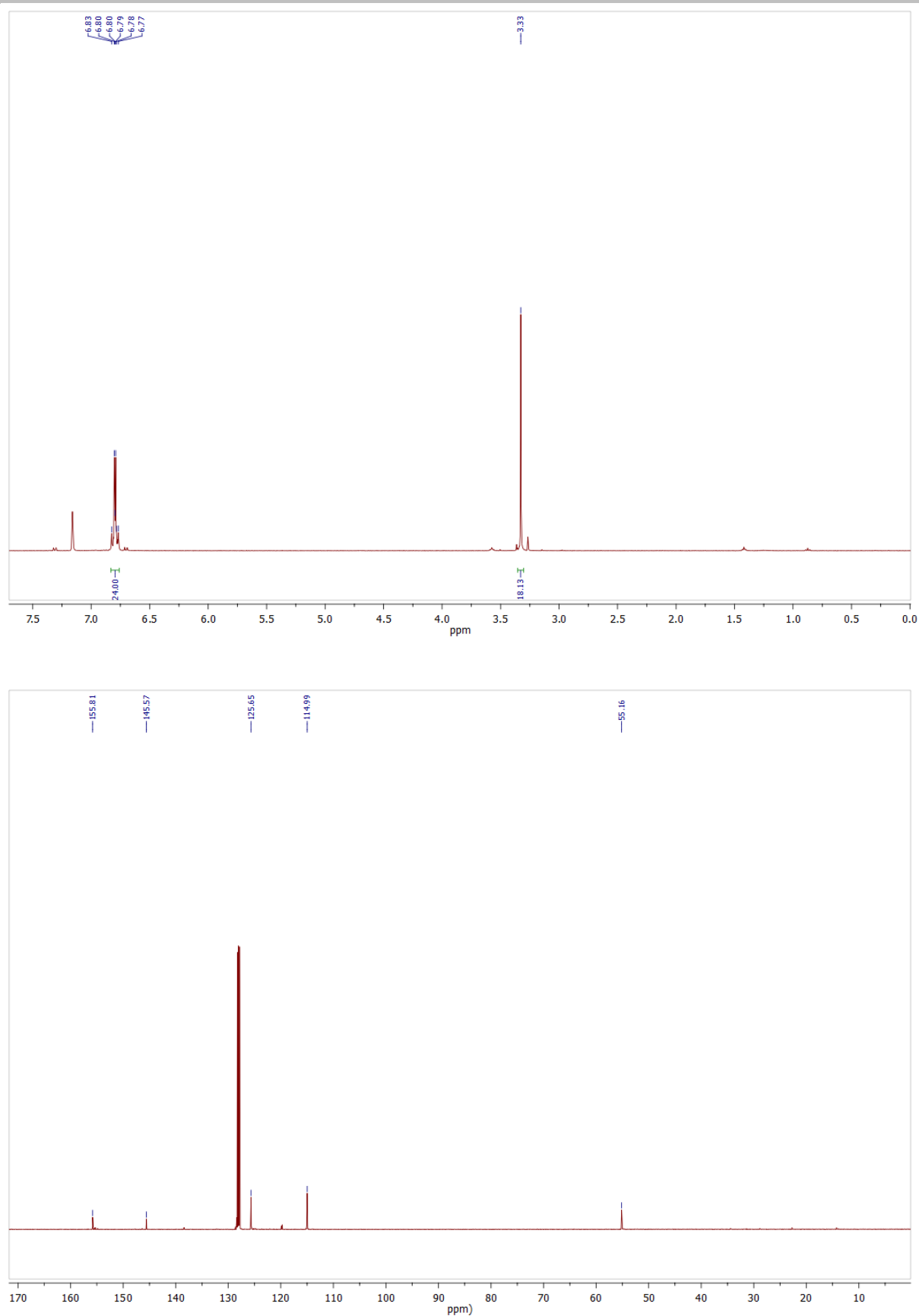


Figure S14. ^1H and ^{13}C spectra of compound 1-OMe in Benzene- d_6 .

SUPPORTING INFORMATION

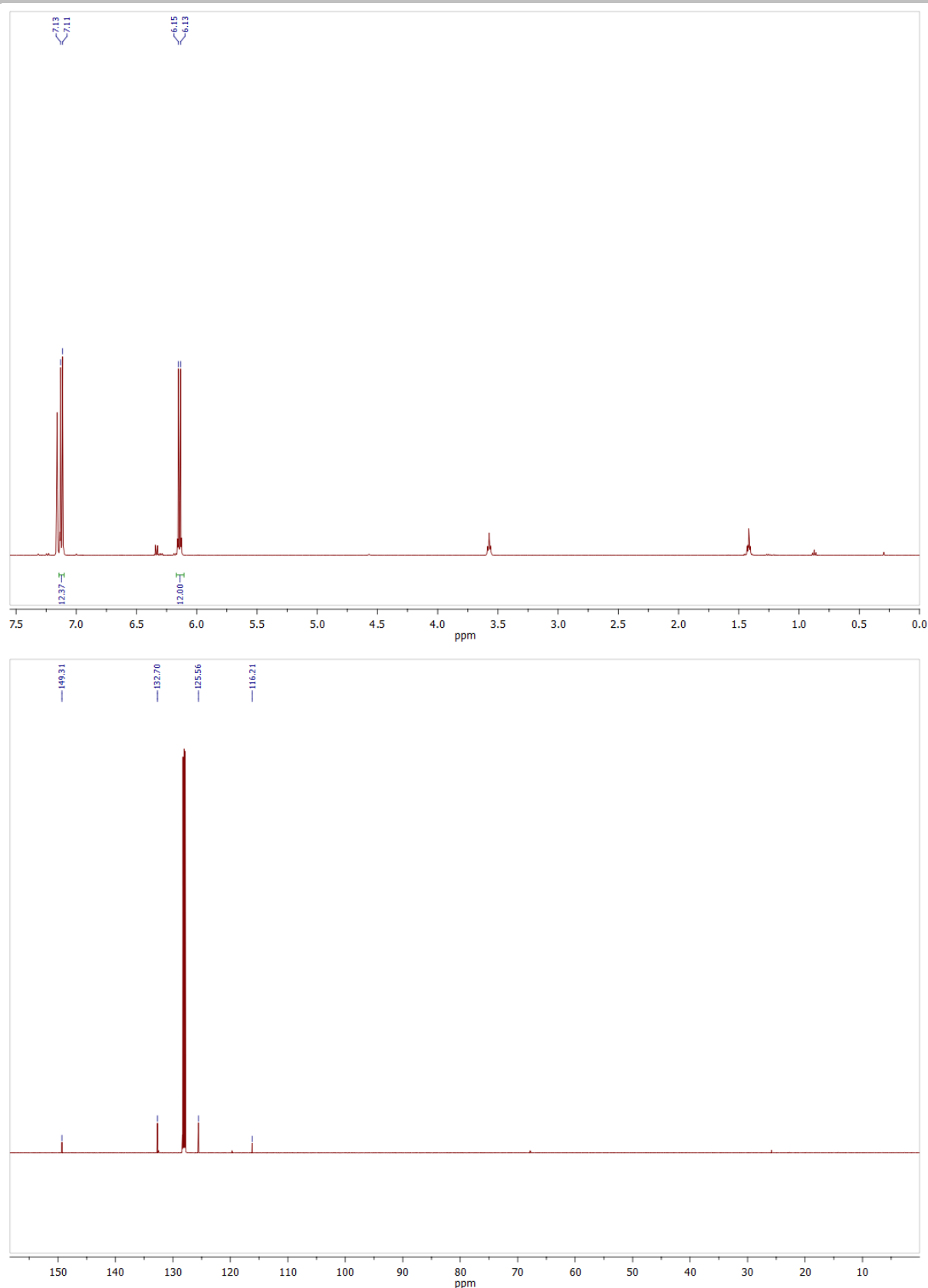


Figure S15. ^1H and ^{13}C spectra of compound **1-Br** in $\text{Benzene-}d_6$.

SUPPORTING INFORMATION

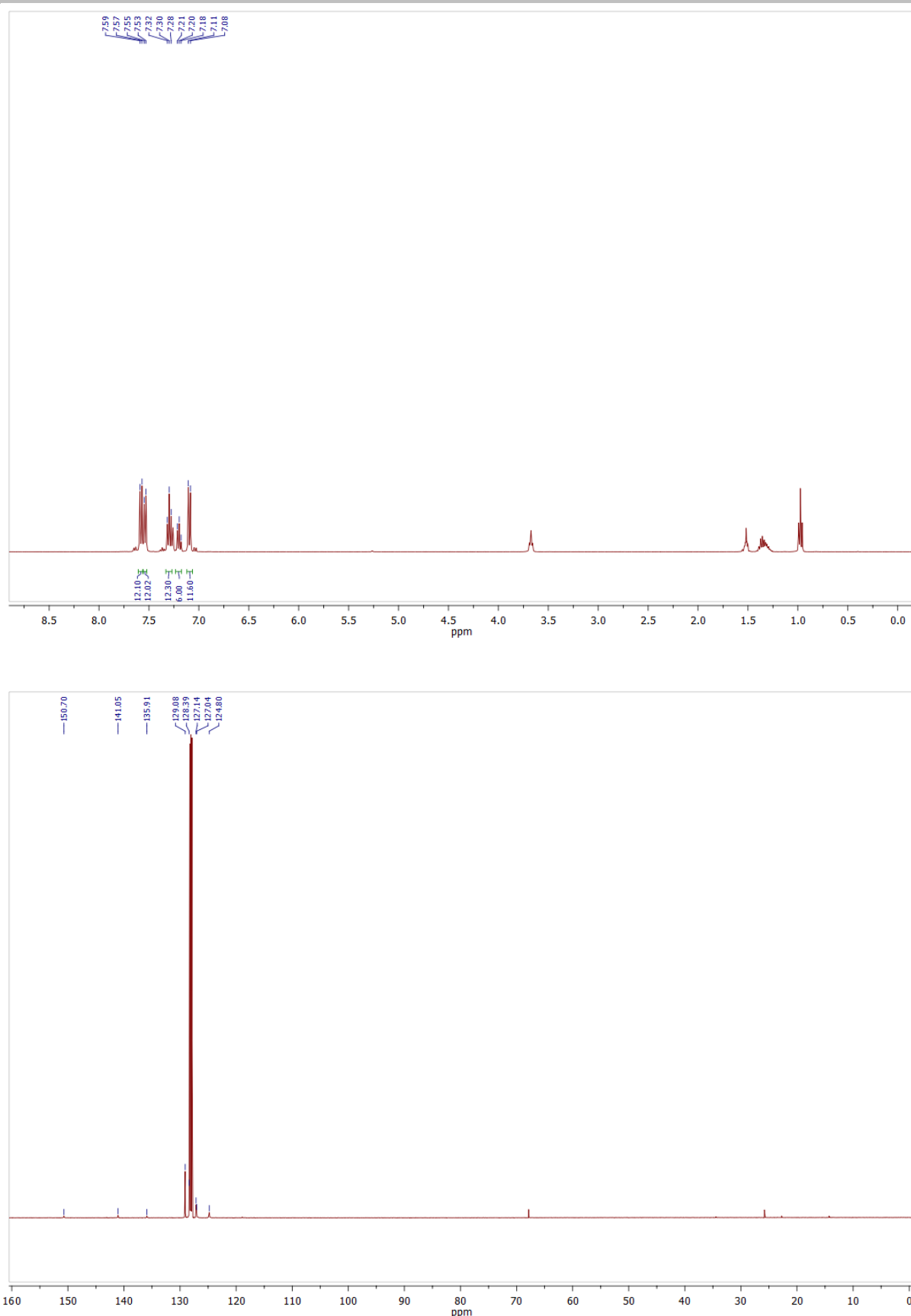


Figure S16. ¹H and ¹³C spectra of compound 1-Ph in Benzene-*d*₆.

SUPPORTING INFORMATION

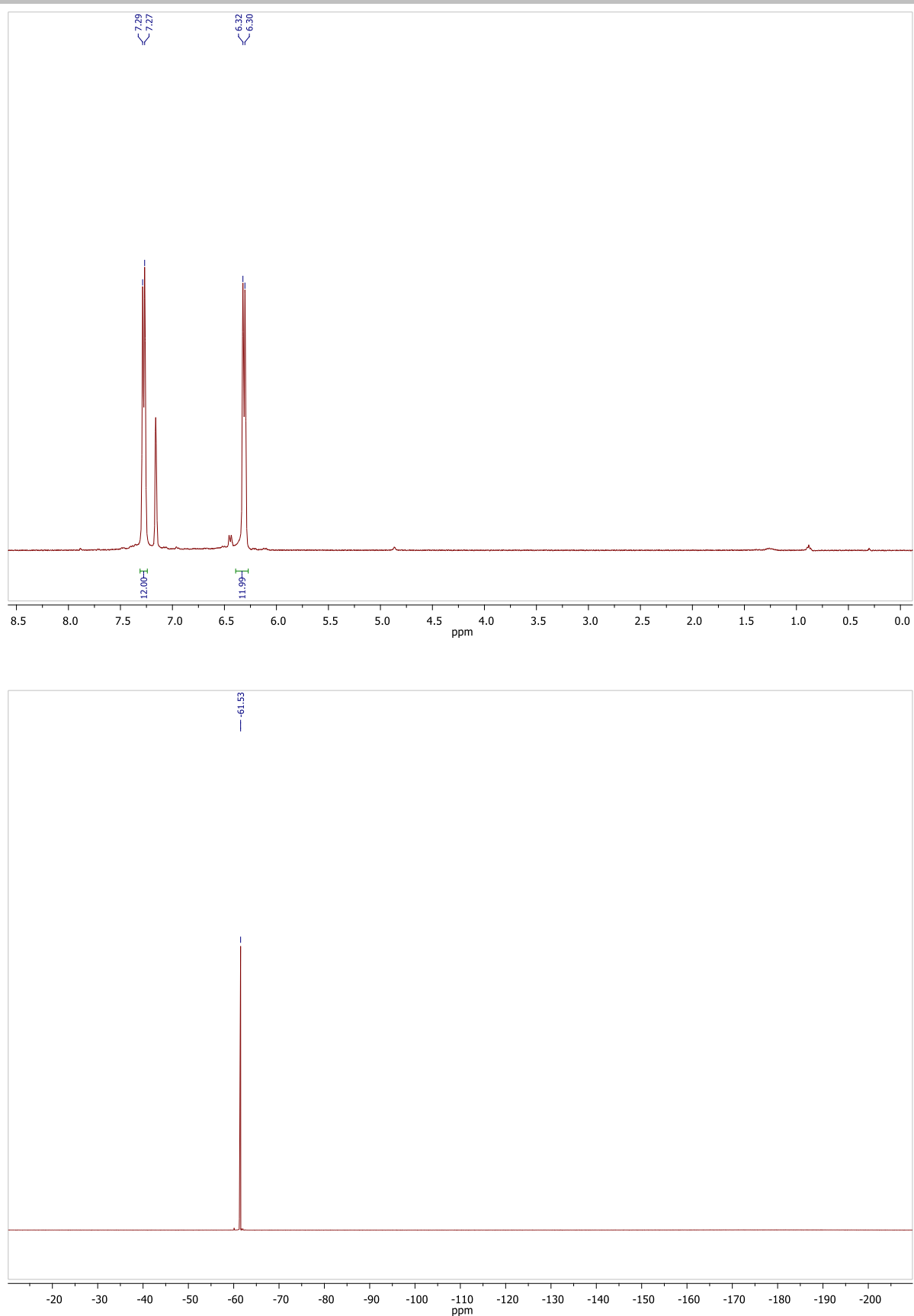


Figure S17. ^1H and ^{19}F spectra of compound **1-CF₃** in Benzene-*d*₆.

SUPPORTING INFORMATION

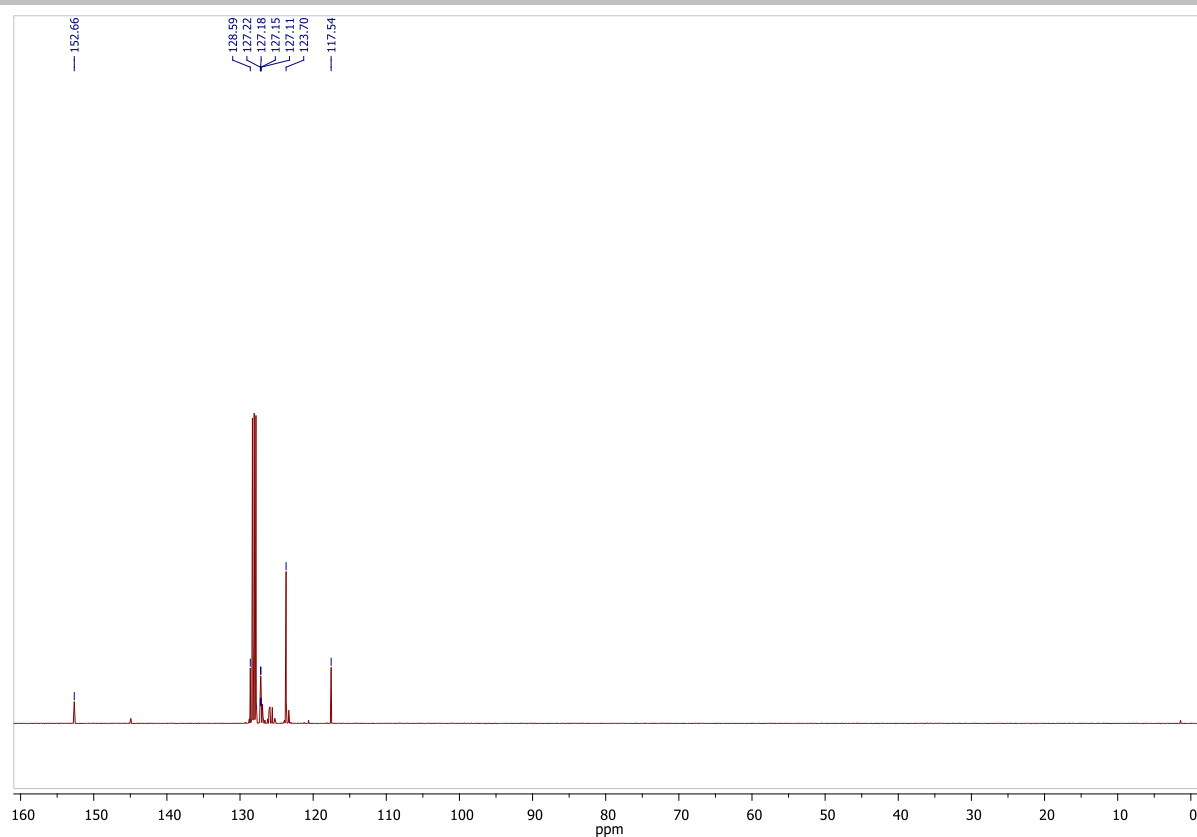


Figure S18. ^{13}C spectrum of compound **1-CF₃** in Benzene-*d*₆.

SUPPORTING INFORMATION

Quantum Chemical Analyses

All DFT calculations were performed with the Amsterdam Density Functional (ADF) program^[26] using relativistic, dispersion-corrected density functional theory (DFT) at the ZORA-BLYP-D3BJ/TZ2P level of theory for geometry optimizations and energy calculations, with the full electron model for all atoms (no frozen core).^{[27],[28]} Solvation in benzene was simulated by using the conductor-like screening model (COSMO).^[29] Bismuth(0) has been calculated as a bulk by means of periodic DFT with the same ADF package (BAND) and at the same ZORA-BLYP(D3BJ)/TZ2P level of theory. All stationary points were verified to be minima on the potential energy surface through vibrational analysis.

The bonding mode in **2-X**, with special emphasis on Bi–NR₂ interactions, was analyzed within the framework of quantitative Kohn-Sham molecular orbital theory^[30] in combination with a quantitative energy decomposition analysis (EDA)^[30] in the gas phase. The electronic bond energy ΔE can be decomposed into the strain energy ΔE_{strain} associated with deforming two fragments (in triplet state) from their equilibrium structure to the geometry they adopt in **2-X** plus the interaction energy ΔE_{int} between these deformed fragments. The latter is further decomposed into the classical electrostatic attraction ΔV_{elstat} , Pauli repulsion ΔE_{Pauli} between occupied orbitals, stabilizing orbital interactions ΔE_{oi} , and dispersion interactions ΔE_{disp} .^[30]

Table S3. Homolytic and heterolytic bond dissociation energies (in kcal mol⁻¹) of bismuth amides in benzene and in the gas phase.^a

System	benzene				gas			
	homolytic		heterolytic		homolytic		heterolytic	
	ΔE	ΔG	ΔE	ΔG	ΔE	ΔG	ΔE	ΔG
1-H	42.6	28.0	77.8	63.8	43.5	27.4	130.7	115.5
1-Me	39.4	25.4	76.3	62.2	40.2	25.0	120.8	105.1
1-OMe	36.1	18.7	74.5	55.2	37.0	19.7	116.1	97.1
1-Ph	47.1	31.9	75.3	59.8	47.6	28.0	113.5	94.6
1-Br	40.1	20.6	77.0	56.0	40.2	19.4	120.1	99.0
1-CF₃	44.5	24.5	78.2	59.9	44.9	26.2	122.6	104.2

^a Computed at the ZORA-BLYP-D3BJ/TZ2P level of theory. Homolytic $\text{Bi}[\text{N}(\text{C}_6\text{H}_4\text{X})_2]_3 \rightarrow \text{Bi}[\text{N}(\text{C}_6\text{H}_4\text{X})_2]_2^{\bullet} + \text{N}(\text{C}_6\text{H}_4\text{X})_2^{\bullet}$ vs. heterolytic $\text{Bi}[\text{N}(\text{C}_6\text{H}_4\text{X})_2]_3 \rightarrow \text{Bi}[\text{N}(\text{C}_6\text{H}_4\text{X})_2]_2^+ + \text{N}(\text{C}_6\text{H}_4\text{X})_2^-$ reactions have been computed.

Table S4. Comparison between homolytic and heterolytic bond dissociation energies (in kcal mol⁻¹) of **1-H** and **1-Me** and their protonated forms in benzene and in the gas phase.^a

System	benzene				gas			
	homolytic		heterolytic		homolytic		heterolytic	
	ΔE	ΔG	ΔE	ΔG	ΔE	ΔG	ΔE	ΔG
1-H	42.6	28.0	77.8	63.8	43.5	27.4	130.7	115.5
1-HH	45.1	29.2	15.5	0.4	55.4	38.8	28.8	13.1
1-Me	39.4	25.4	76.3	62.2	40.2	25.0	120.8	105.1
1-MeH	44.6	28.7	18.8	4.6	51.0	40.4	22.4	11.7

^a Computed at the ZORA-BLYP-D3BJ/TZ2P level of theory. Homolytic $[\text{Bi}(\text{N}(\text{C}_6\text{H}_4\text{X})_2)_2(\text{HN}(\text{C}_6\text{H}_4\text{X})_2)]^+ \rightarrow [\text{Bi}(\text{N}(\text{C}_6\text{H}_4\text{X})_2)_2^{\bullet} + [\text{HN}(\text{C}_6\text{H}_4\text{X})_2]^{\bullet+}$ vs. heterolytic $[\text{Bi}(\text{N}(\text{C}_6\text{H}_4\text{X})_2)_2(\text{HN}(\text{C}_6\text{H}_4\text{X})_2)]^+ \rightarrow [\text{Bi}(\text{N}(\text{C}_6\text{H}_4\text{X})_2)_2^+ + \text{HN}(\text{C}_6\text{H}_4\text{X})_2]$ have been computed

Table S5. Energy decomposition analysis (in kcal mol⁻¹) in the gas phase of the homolytic Bi–N bond energy ΔE for bismuth amides optimized in benzene with COSMO.

System	ΔE_{Pauli}	ΔV_{elstat}	ΔE_{oi}	ΔE_{disp}	ΔE_{int}	ΔE_{strain}	ΔE
1-OMe	256.5	-144.4	-136.0	-28.0	-51.9	15.0	-36.9
1-Me	251.5	-140.7	-135.8	-28.4	-53.3	13.2	-40.1
1-H	249.5	-138.6	-137.7	-29.3	-56.1	12.7	-43.4
1-Ph	261.7	-143.4	-131.4	-49.6	-62.7	15.1	-47.6
1-Br	245.7	-136.4	-134.4	-29.3	-54.4	14.3	-40.2
1-CF₃	240.0	-130.8	-135.4	-29.6	-55.7	11.1	-44.7

^a Computed at ZORA-BLYP-D3BJ/TZ2P//COSMO(benzene)-ZORA-BLYP-D3BJ/TZ2P.

SUPPORTING INFORMATION

Table S6. Thermodynamics (in kcal mol⁻¹) of the elimination of **3-Me** from **1-Me** with formation of different types of bismuthinidenes (triplet [³[Bi(NR₂)]] vs. singlet [¹[Bi(NR₂)]] and benzene adducts of the triplet bismuthinidene (³[Bi(NR₂)(benzene)]) and ³[Bi(NR₂)(benzene)₂])) computed at ZORA-BLYP(D3BJ/TZ2P level of theory in benzene.

System	ΔH	ΔG
1-Me → ³ [Bi(NR ₂)] + 3-Me	57.4	46.3
1-Me → ¹ [Bi(NR ₂)] ^a + 3-Me	67.2	54.3
1-Me + benzene → ³ [Bi(NR ₂)](benzene) + 3-Me	52.1	50.6
1-Me + 2 benzene → ³ [Bi(NR ₂)](benzene) ₂ + 3-Me	44.8	53.3

^a The singlet ¹[Bi(NR₂)] was computed as a single point on the geometry of ³[Bi(NR₂)] due to non-convergency.

[Bi(NR₂)] is more stable at its triplet state than its singlet state by about 7 kcal mol⁻¹ (when referring to ΔG). This difference is kept when one benzene molecule is included as a discrete model of solvation, but it is decreased when two benzene molecules are included to become almost isoenergetic (data not included in Table S6). In any case, the high energies corresponding to the formation of this bismuthinidene in the reaction **1-Me** → **3-Me** + [Bi(NR₂)] make this reaction pathway highly unlikely to contribute to the experimentally observed formation **3-Me** from **1-Me**.

Rationale of radical catalysis. As outlined in the main part of this work, we suggest that the single steps proposed for the formation of **3-Me** from **1-Me** (and related reactions) may well proceed through catalysis by radicals such as (NR₂)[•]. Scheme S2 provides a rationale for this suggestion for the reaction of [Bi(NR₂)₃] to give [Bi₂(NR₂)₄]. Homolytic Bi–N bond dissociation of **1-Me** (ΔG = 25.4 kcal·mol⁻¹) or [Bi₂(NR₂)₄] (ΔG = 28.9 kcal·mol⁻¹) would readily provide sufficient concentrations of such radical species. These results suggest that multiple sources of radicals (NR₂)[•] are possible. EPR spectroscopic experiments showed that these radicals are present in the reaction mixture and do not originate from N–N bond hemolysis of **3-Me**.



Scheme S2. Rationale of radical catalysis in reactions of [Bi(NR₂)₃] to give (NR₂)₂.

Table S7. Cartesian coordinates and ADF total electronic and Gibbs energies (in parentheses and in kcal mol⁻¹) of compounds **1-X** under analysis computed at the ZORA-BLYP(D3BJ/TZ2P level of theory in benzene.

1-H (-10208.8, -9911.1)							
1.Bi	1.019609	8.973795	9.961489	36.H	-3.729453	6.448128	8.417295
2.N	-0.463314	7.907714	11.278511	37.C	-1.602781	5.730330	11.229109
3.C	0.736260	5.853365	11.844803	38.H	-2.527592	6.224862	10.948963
4.H	1.622053	6.440790	12.063102	39.C	2.305459	6.664420	6.858640
5.C	-1.072224	8.374801	7.475434	40.H	3.148482	7.347322	6.796074
6.C	-2.836600	10.733697	11.831957	41.C	1.666556	6.483836	8.094380
7.H	-3.147562	11.642585	11.321908	42.C	-3.037077	6.659025	6.382623
8.C	-1.111382	8.109546	6.089636	43.H	-3.788303	5.995008	5.962819
9.H	-0.356500	8.545756	5.443639	44.C	-2.086763	7.270599	5.555496
10.C	-2.039557	7.767754	8.298527	45.H	-2.087716	7.072034	4.485889
11.H	-2.030239	7.961839	9.362046	46.C	-1.901948	9.893762	11.218947
12.C	1.556497	12.480594	5.877772	47.H	-1.543689	10.144871	10.222558
13.H	1.969052	13.336182	5.349572	48.C	0.129819	4.924127	7.051121
14.C	0.574356	5.609835	8.183993	49.H	-0.729186	4.263308	7.128159
15.H	0.076500	5.473836	9.136296	50.C	-1.551337	4.340487	11.327870
16.C	0.772164	5.100972	5.822717	51.H	-2.446332	3.756062	11.126587
17.H	0.417161	4.574589	4.940345	52.C	0.790073	4.459996	11.918562
18.C	-0.371903	11.204397	6.627334	53.H	1.727407	3.976654	12.181228
19.H	-1.448211	11.071114	6.692095	54.N	-0.063203	9.197915	8.017155
20.C	-0.450383	6.505774	11.472613	55.C	0.473196	10.260752	7.253193
21.C	-1.469561	8.704265	11.850164	56.C	3.233497	6.698323	9.959154
22.C	-2.996396	9.201142	13.687863	57.C	4.950308	6.985067	11.681366
23.H	-3.423121	8.920946	14.648615	58.H	5.437291	7.627586	12.411568
24.N	2.141334	7.202104	9.240859	59.C	3.903124	7.497546	10.915866
25.C	-2.046794	8.369564	13.098860	60.H	3.616361	8.539062	11.056070
26.H	-1.733803	7.457921	13.598861	61.C	1.861402	5.974528	5.728298
27.C	-3.394202	10.395184	13.067532	62.H	2.358887	6.126745	4.773232
28.H	-4.132723	11.040544	13.535515	63.C	3.690897	5.371952	9.779954
29.C	0.166382	12.291279	5.942963	64.H	3.196493	4.733007	9.056420
30.H	-0.500971	13.007950	5.469241	65.C	-0.351468	3.695330	11.658637
31.C	1.868499	10.441936	7.154903	66.H	-0.310987	2.610618	11.716285
32.H	2.535630	9.683633	7.559545	67.C	4.750926	4.874700	10.538778
33.C	2.401937	11.552873	6.489719	68.H	5.074867	3.847991	10.380579
34.H	3.481191	11.673001	6.430184	69.C	5.386863	5.666767	11.502188
35.C	-2.999868	6.912446	7.757434	70.H	6.207816	5.270556	12.093595

SUPPORTING INFORMATION

1-Me (-12418.9, -12027.3)				1-OMe (-13234.3, -12829.2)			
1.Bi	3.238724	9.309538	4.995706	71.C	-3.569602	11.455249	5.205376
2.N	2.868870	7.284791	5.831294	72.H	-4.406165	10.972028	4.686524
3.N	4.749996	8.643833	3.509799	73.H	-3.619744	12.528222	4.971699
4.N	1.528204	9.258797	3.577625	74.H	-3.729786	11.346118	6.283641
5.C	3.578396	6.868259	6.965237	75.C	1.680062	8.720951	2.261601
6.C	4.726562	7.560703	7.414350	76.C	2.374911	9.427587	1.271938
7.H	5.119280	8.403452	6.847440	77.H	2.801969	10.396813	1.508044
8.C	5.410305	7.167741	8.565763	78.C	2.532599	8.887866	-0.007395
9.H	6.290905	7.731036	8.870317	79.H	3.088292	9.448367	-0.756769
10.C	5.007994	6.053728	9.316934	80.C	1.991328	7.636108	-0.338407
11.C	3.880481	5.351712	8.859794	81.C	1.280731	6.943552	0.656625
12.H	3.538589	4.475549	9.409500	82.H	0.852692	5.968708	0.429685
13.C	3.175251	5.741597	7.721943	83.C	1.129177	7.471340	1.937842
14.H	2.305438	5.173928	7.408593	84.H	0.584255	6.922263	2.695841
15.C	5.742935	5.633592	10.571737	85.C	2.202135	7.030943	-1.708833
16.H	5.839537	4.542888	10.632429	86.H	1.338867	6.430980	-2.017382
17.H	5.211336	5.962468	11.475883	87.H	3.078770	6.368194	-1.712561
18.H	6.748893	6.066090	10.606279	88.H	2.373339	7.804729	-2.464584
19.C	1.886866	6.416468	5.260586				
20.C	2.283626	5.300246	4.507213				
21.H	3.340113	5.107839	4.367590				
22.C	1.331065	4.457104	3.938991				
23.H	1.660886	3.607297	3.343891				
24.C	-0.044596	4.699182	4.097369				
25.C	-0.431480	5.815394	4.853693				
26.H	-1.489123	6.035762	4.984163				
27.C	0.519117	6.660006	5.434475				
28.H	0.198393	7.522051	6.010164				
29.C	-1.070967	3.778389	3.474919				
30.H	-2.054021	4.257168	3.420106				
31.H	-1.181780	2.857292	4.063326				
32.H	-0.775525	3.481272	2.461881				
33.C	5.480808	9.597856	2.789571				
34.C	5.103151	10.960497	2.773407				
35.H	4.199382	11.288694	3.284748				
36.C	5.851397	11.915625	2.085087				
37.H	5.520936	12.952971	2.103032				
38.C	6.998591	11.567318	1.356572				
39.C	7.369679	10.213033	1.363523				
40.H	8.257359	9.900376	0.814862				
41.C	6.642393	9.248415	2.060282				
42.H	6.972147	8.214938	2.047905				
43.C	7.777934	12.595913	0.565770				
44.H	8.850810	12.370522	0.567679				
45.H	7.640392	13.602176	0.976852				
46.H	7.453592	12.623220	-0.484461				
47.C	5.006191	7.254304	3.293395				
48.C	4.557378	6.626329	2.121373				
49.H	4.021022	7.209907	1.383281				
50.C	4.797130	5.269448	1.911199				
51.H	4.430298	4.799625	1.000338				
52.C	5.483313	4.494284	2.861373				
53.C	5.937087	5.133068	4.025530				
54.H	6.472307	4.559128	4.779602				
55.C	5.707710	6.495084	4.238383				
56.H	6.064486	6.969785	5.146654				
57.C	5.685739	3.009329	2.655113				
58.H	6.552826	2.643348	3.214993				
59.H	5.830974	2.769446	1.595968				
60.H	4.808935	2.444126	3.000755				
61.C	0.285915	9.772237	3.972295				
62.C	0.013974	10.094060	5.322030				
63.H	0.753671	9.897325	6.096555				
64.C	-1.212756	10.633511	5.710044				
65.H	-1.375812	10.861009	6.762307				
66.C	-2.242490	10.861051	4.785484				
67.C	-1.980399	10.526223	3.446994				
68.H	-2.755040	10.680606	2.696805				
69.C	-0.754029	10.002473	3.039813				
70.H	-0.593804	9.763149	1.993911				

SUPPORTING INFORMATION

13.C	3.882751	5.182234	6.978812		84.H	-1.077900	7.615600	2.760932
14.H	3.174080	4.455217	6.600562		85.C	0.781241	4.386860	-0.086832
15.C	7.142792	5.155923	9.000771		86.H	0.453233	3.494861	0.463773
16.H	7.417438	4.133527	8.721275		87.H	1.742613	4.156918	-0.556172
17.H	6.920604	5.154381	10.076714		88.H	0.044883	4.562973	-0.879720
18.H	8.013877	5.802163	8.847931		89.H	5.783471	8.200270	5.100328
19.C	1.594280	6.151995	5.462927					
20.C	1.846385	5.139833	4.524887					
21.H	2.848659	5.015904	4.129667					
22.C	0.810032	4.318498	4.087892					
23.H	1.020982	3.539452	3.359384					
24.C	-0.504812	4.498798	4.547006					
25.C	-0.746063	5.522331	5.474853					
26.H	-1.755727	5.682586	5.846656					
27.C	0.289830	6.339776	5.933847					
28.H	0.095231	7.123278	6.661737					
29.C	-1.631729	3.648884	4.009434					
30.H	-2.493539	3.651179	4.684015					
31.H	-1.312855	2.612280	3.855944					
32.H	-1.969508	4.033105	3.036988					
33.C	5.751412	9.809932	3.834907					
34.C	5.001397	10.504146	2.872705					
35.H	4.195027	10.004396	2.340822					
36.C	5.299829	11.835823	2.584272					
37.H	4.713281	12.359136	1.832738					
38.C	6.333212	12.512744	3.254151					
39.C	7.057170	11.808829	4.228357					
40.H	7.857076	12.310079	4.768314					
41.C	6.777568	10.470013	4.516454					
42.H	7.359074	9.939369	5.267250					
43.C	6.666688	13.947093	2.914947					
44.H	7.178119	14.444644	3.744657					
45.H	5.764923	14.517576	2.668565					
46.H	7.330782	13.991384	2.041338					
47.C	5.567517	7.365866	3.264821					
48.C	5.795015	7.556000	1.898280					
49.H	5.918010	8.552339	1.490014					
50.C	5.873178	6.447735	1.048837					
51.H	6.048257	6.613034	-0.011725					
52.C	5.732351	5.139096	1.528991					
53.C	5.535293	4.969884	2.910806					
54.H	5.442163	3.966759	3.321697					
55.C	5.451557	6.061423	3.769593					
56.H	5.294854	5.902996	4.831695					
57.C	5.777372	3.947255	0.601081					
58.H	4.802340	3.443655	0.562298					
59.H	6.507943	3.205042	0.943885					
60.H	6.043678	4.245058	-0.417366					
61.C	0.323219	9.929316	3.496111					
62.C	-0.165737	10.536633	4.669866					
63.H	-0.007165	10.048027	5.629434					
64.C	-0.912593	11.717025	4.601267					
65.H	-1.279970	12.167492	5.520431					
66.C	-1.229949	12.301359	3.369106					
67.C	-0.763368	11.667554	2.196874					
68.H	-0.995953	12.105111	1.227961					
69.C	0.003366	10.511006	2.249426					
70.H	0.374619	10.053045	1.337193					
71.C	-2.068254	13.554530	3.281304					
72.H	-3.038618	13.343748	2.813284					
73.H	-1.573801	14.316219	2.666102					
74.H	-2.255473	13.980160	4.271510					
75.C	1.074038	7.751280	2.641326					
76.C	2.224142	7.213257	2.047555					
77.H	3.194948	7.649600	2.259257					
78.C	2.131186	6.134149	1.168695					
79.H	3.040691	5.733208	0.730101					
80.C	0.889737	5.576273	0.837990					
81.C	-0.262469	6.147900	1.410530					
82.H	-1.239377	5.735015	1.167946					
83.C	-0.181276	7.211566	2.301218					

SUPPORTING INFORMATION

Table S8. Cartesian coordinates and ADF total electronic and Gibbs energies (in parentheses and in kcal mol⁻¹) of compounds **1-X** under analysis computed at the ZORA-BLYP(D3BJ)/TZ2P level of theory in the gas phase.

1-H (-10205.8, -9907.8)				1-Me (-12416.35, -12023.1)			
1.Bi	1.008864	8.966165	9.952143	67.C	4.719707	4.877994	10.577941
2.N	-0.457437	7.899634	11.277174	68.H	5.029876	3.844019	10.441267
3.C	0.733784	5.836472	11.829577	69.C	5.361682	5.678642	11.529349
4.H	1.624238	6.417504	12.045908	70.H	6.172899	5.281387	12.133074
5.C	-1.079180	8.374652	7.470927				
6.C	-2.823352	10.728397	11.851306				
7.H	-3.142319	11.634841	11.341928				
8.C	-1.107643	8.102800	6.086869				
9.H	-0.347907	8.536229	5.444710				
10.C	-2.052522	7.774802	8.291144				
11.H	-2.053591	7.977930	9.353163				
12.C	1.549130	12.483583	5.877724				
13.H	1.961852	13.339573	5.350457				
14.C	0.579296	5.623216	8.175316				
15.H	0.077774	5.497773	9.127065				
16.C	0.783501	5.089543	5.820775				
17.H	0.429753	4.555053	4.942784				
18.C	-0.379355	11.206113	6.622790				
19.H	-1.455346	11.069272	6.684505				
20.C	-0.450518	6.496573	11.464908				
21.C	-1.457815	8.699474	11.858013				
22.C	-2.957160	9.202885	13.713901				
23.H	-3.370982	8.926605	14.681373				
24.N	2.153212	7.219099	9.220274				
25.C	-2.016617	8.368953	13.115302				
26.H	-1.695646	7.458729	13.612713				
27.C	-3.362384	10.394670	13.095236				
28.H	-4.093838	11.041919	13.571447				
29.C	0.159621	12.292741	5.939648				
30.H	-0.507119	13.008482	5.463626				
31.C	1.860676	10.445352	7.154272				
32.H	2.526278	9.684401	7.556797				
33.C	2.393960	11.556767	6.490264				
34.H	3.473211	11.6777615	6.431245				
35.C	-3.009889	6.918361	7.747321				
36.H	-3.746875	6.460864	8.403630				
37.C	-1.608947	5.729616	11.224735				
38.H	-2.531403	6.232416	10.951669				
39.C	2.321077	6.654770	6.846040				
40.H	3.168876	7.331405	6.781002				
41.C	1.676343	6.490436	8.080775				
42.C	-3.037374	6.658004	6.374092				
43.H	-3.788381	5.995202	5.952192				
44.C	-2.081100	7.263529	5.550395				
45.H	-2.076735	7.061329	4.481529				
46.C	-1.898404	9.885638	11.227543				
47.H	-1.559068	10.129357	10.222711				
48.C	0.135363	4.928898	7.047958				
49.H	-0.727448	4.273774	7.129140				
50.C	-1.565380	4.339564	11.319584				
51.H	-2.464977	3.760949	11.121919				
52.C	0.779054	4.442886	11.899142				
53.H	1.714899	3.953899	12.156158				
54.N	-0.072772	9.202002	8.014688				
55.C	0.465378	10.264152	7.250887				
56.C	3.235355	6.711519	9.954632				
57.C	4.947298	7.006818	11.678777				
58.H	5.442533	7.656210	12.397163				
59.C	3.913838	7.520292	10.895716				
60.H	3.647668	8.571164	11.005280				
61.C	1.877899	5.955376	5.721622				
62.H	2.381050	6.093608	4.767403				
63.C	3.671271	5.375530	9.804104				
64.H	3.169901	4.731472	9.090057				
65.C	-0.368163	3.686571	11.642547				
66.H	-0.334270	2.601530	11.697377				

SUPPORTING INFORMATION

18.C	10.250877	-10.229008	-0.837782	89.C	16.259222	-11.252170	-10.087399
19.H	9.656837	-9.394964	-0.471382	90.C	17.632922	-11.005326	-10.291766
20.C	9.931375	-11.536758	-0.457730	91.H	18.341779	-11.258043	-9.515247
21.H	9.085891	-11.726789	0.198783	92.C	18.097683	-10.421693	-11.464028
22.C	10.710992	-12.598314	-0.929941	93.H	19.165453	-10.251426	-11.574601
23.H	10.467908	-13.620230	-0.647797	94.C	17.224456	-10.063005	-12.507151
24.C	11.793887	-12.353793	-1.776133	95.C	15.858237	-10.351305	-12.321042
25.H	12.371202	-13.190266	-2.161810	96.H	15.146080	-10.089283	-13.099740
26.C	16.720593	-8.891636	-6.413369	97.C	15.381136	-10.929191	-11.148688
27.C	17.141957	-8.705860	-7.740303	98.H	14.319065	-11.125435	-11.044132
28.H	17.133943	-9.536427	-8.435121	99.C	17.719928	-9.399846	-13.734547
29.C	17.606776	-7.472566	-8.182752	100.C	17.143694	-9.663415	-14.992907
30.H	17.969669	-7.392626	-9.203169	101.H	16.339767	-10.391033	-15.069804
31.C	17.644776	-6.353577	-7.331896	102.C	17.609286	-9.027810	-16.145383
32.C	17.189994	-6.537957	-6.010438	103.H	17.152436	-9.254133	-17.106318
33.H	17.180787	-5.694133	-5.325635	104.C	18.666025	-8.114025	-16.070734
34.C	16.744654	-7.773067	-5.553873	105.H	19.028822	-7.619530	-16.968464
35.H	16.422709	-7.884113	-4.522903	106.C	19.251073	-7.842793	-14.829260
36.C	18.143462	-5.039592	-7.796462	107.H	20.067645	-7.127660	-14.756854
37.C	17.984220	-4.632486	-9.135526	108.C	18.782799	-8.475973	-13.676786
38.H	17.466203	-5.283122	-9.835130	109.H	19.227402	-8.234626	-12.714561
39.C	18.452112	-3.391537	-9.570956	110.C	14.475970	-11.616924	-8.445505
40.H	18.309255	-3.097031	-10.608343	111.C	13.844485	-10.355153	-8.496320
41.C	19.086060	-2.523271	-8.676813	112.H	14.346699	-9.528820	-8.989388
42.H	19.449605	-1.555960	-9.014985	113.C	12.625387	-10.150189	-7.865408
43.C	19.255783	-2.915337	-7.345380	114.H	12.189115	-9.154779	-7.879463
44.H	19.771154	-2.261711	-6.646548	115.C	11.984922	-11.173413	-7.131919
45.C	18.795058	-4.157583	-6.912768	116.C	12.603181	-12.434493	-7.106392
46.H	18.977994	-4.464855	-5.887424	117.H	12.119495	-13.259181	-6.590480
47.C	19.797240	-10.545055	-7.234252	118.C	13.814888	-12.658577	-7.759621
48.C	19.706822	-9.719269	-6.102170	119.H	14.256831	-13.652967	-7.766391
49.H	19.157807	-10.070854	-5.233489	120.C	10.741753	-10.909285	-6.374333
50.C	20.262122	-8.443257	-6.107535	121.C	9.788706	-9.975575	-6.826440
51.H	20.124599	-7.806074	-5.239424	122.H	9.934439	-9.479520	-7.782558
52.C	20.942763	-7.945864	-7.233277	123.C	8.645672	-9.697456	-6.074571
53.C	21.070061	-8.799250	-8.347136	124.H	7.919607	-8.977788	-6.446112
54.H	21.620833	-8.460018	-9.220275	125.C	8.429419	-10.344270	-4.852530
55.C	20.510244	-10.071080	-8.352624	126.H	7.543547	-10.119962	-4.263401
56.H	20.618034	-10.707447	-9.225989	127.C	9.364000	-11.277201	-4.392319
57.C	21.497027	-6.573211	-7.259824	128.H	9.222934	-11.767732	-3.433241
58.C	21.497455	-5.820148	-8.449995	129.C	10.502983	-11.556982	-5.146580
59.H	21.042980	-6.235066	-9.344883	130.H	11.241663	-12.248056	-4.754771
60.C	22.029377	-4.532526	-8.485390				
61.H	21.996940	-3.963206	-9.410372				
62.C	22.569523	-3.961240	-7.329266				
63.H	22.979170	-2.954563	-7.355726				
64.C	22.565301	-4.689739	-6.136268				
65.H	22.985575	-4.256431	-5.231328				
66.C	22.035076	-5.981000	-6.102023				
67.H	22.064166	-6.548380	-5.175385				
68.C	19.773710	-12.911749	-7.858341				
69.C	21.134905	-13.177644	-7.591392				
70.H	21.698932	-12.478233	-6.981285				
71.C	21.749888	-14.313603	-8.101892				
72.H	22.804547	-14.477670	-7.895933				
73.C	21.046163	-15.247762	-8.892454				
74.C	19.695273	-14.975916	-9.161194				
75.H	19.117743	-15.667318	-9.768858				
76.C	19.073903	-13.824902	-8.673880				
77.H	18.048912	-13.620188	-8.979489				
78.C	21.712574	-16.457406	-9.430334				
79.C	22.676933	-17.150010	-8.672865				
80.H	22.916503	-16.805868	-7.669962				
81.C	23.306389	-18.288590	-9.179090				
82.H	24.042080	-18.811520	-8.572196				
83.C	22.986195	-18.763224	-10.455338				
84.H	23.476891	-19.649543	-10.849960				
85.C	22.030138	-18.086322	-11.219854				
86.H	21.780722	-18.439914	-12.217739				
87.C	21.402019	-16.946901	-10.714007				
88.H	20.682186	-16.413503	-11.329584				

SUPPORTING INFORMATION

28.H	6.922821	2.697896	22.980374	27.C	0.509323	6.666787	5.425514
29.C	4.989342	3.088520	22.114739	28.H	0.176486	7.521291	6.004287
30.H	5.089760	2.248030	21.429682	29.C	-0.993343	3.853467	3.351661
31.C	5.021904	4.265901	18.849791	30.F	-2.260111	3.966204	3.847902
32.H	5.600644	3.717523	19.585407	31.F	-0.655045	2.529245	3.389680
33.C	3.996905	3.617435	18.147556	32.F	-1.060111	4.200356	2.015211
34.C	4.542557	6.316124	17.683377	33.C	5.472612	9.608654	2.823861
35.C	5.297003	5.618523	18.627835	34.C	5.079431	10.968201	2.814657
36.H	6.079484	6.119051	19.189026	35.H	4.180800	11.290069	3.338708
37.C	3.534315	5.685258	16.950806	36.C	5.801118	11.928499	2.114811
38.H	2.954510	6.237157	16.217889	37.H	5.472644	12.963145	2.129674
39.C	4.064368	1.270043	17.463614	38.C	6.935316	11.563403	1.379707
40.C	3.266946	4.337815	17.189083	39.C	7.332134	10.219600	1.365287
41.H	2.486738	3.837266	16.630474	40.H	8.211197	9.921684	0.801483
42.C	4.988432	1.556190	16.431549	41.C	6.623194	9.258748	2.077529
43.H	5.407758	2.552940	16.348948	42.H	6.960510	8.228637	2.063927
44.C	5.375599	0.577956	15.516167	43.C	7.670705	12.585347	0.559754
45.H	6.084667	0.824538	14.731650	44.F	9.003012	12.293360	0.432319
46.C	4.858464	-0.714277	15.615992	45.F	7.581031	13.845584	1.093124
47.C	3.945870	-1.032089	16.621305	46.F	7.170375	12.674393	-0.724140
48.H	3.530504	-2.032511	16.692369	47.C	5.015180	7.263924	3.333666
49.C	3.546790	-0.044997	17.522660	48.C	4.587427	6.656728	2.142203
50.H	2.796306	-0.313380	18.264618	49.H	4.087577	7.255286	1.392377
51.C	0.373419	2.523683	18.183076	50.C	4.807803	5.301191	1.921651
52.C	0.673966	1.841595	16.996015	51.H	4.465814	4.842098	0.999142
53.H	1.062500	0.829757	17.040328	52.C	5.461700	4.533279	2.895471
54.C	0.496747	2.455975	15.752772	53.C	5.907372	5.132918	4.078638
55.H	0.749407	1.928741	14.838491	54.H	6.419622	4.541642	4.830715
56.C	0.001818	3.760262	15.707306	55.C	5.690346	6.495561	4.290600
57.C	-0.330524	4.451273	16.874851	56.H	6.039790	6.961779	5.205102
58.H	-0.715352	5.464929	16.827561	57.C	5.604830	3.045622	2.690811
59.C	-0.140997	3.827606	18.107551	58.F	6.596786	2.500196	3.454246
60.H	-0.390988	4.352629	19.020381	59.F	5.865036	2.721345	1.388755
61.C	-0.505973	1.449260	20.198464	60.F	4.437856	2.386904	3.031182
62.C	-1.782808	1.292554	19.610083	61.C	0.284286	9.774253	3.963140
63.H	-1.927371	1.551480	18.566781	62.C	0.007139	10.099380	5.312401
64.C	-2.862462	0.805123	20.346067	63.H	0.739250	9.899256	6.093156
65.H	-3.832869	0.695634	19.871233	64.C	-1.212959	10.647138	5.691984
66.C	-2.690740	0.450852	21.685051	65.H	-1.393507	10.883169	6.736171
67.C	-1.446776	0.595724	22.298324	66.C	-2.216698	10.864099	4.740396
68.H	-1.314822	0.337735	23.344469	67.C	-1.965852	10.535152	3.401662
69.C	-0.374830	1.103091	21.563683	68.H	-2.735200	10.696105	2.652360
70.H	0.569298	1.252286	22.085432	69.C	-0.740767	10.003954	3.014588
1-CF₃ (-12578.5, -12276.4)							
1.Bi	3.222584	9.315153	5.018416	71.C	-3.522525	11.491052	5.140071
2.N	2.847513	7.294058	5.862057	72.F	-4.564633	11.072830	4.354789
3.N	4.762402	8.652482	3.558038	73.F	-3.488928	12.866672	5.036376
4.N	1.527805	9.259087	3.581812	74.F	-3.859031	11.213421	6.440587
5.C	3.574036	6.867742	6.979067	75.C	1.688221	8.708417	2.272382
6.C	4.709114	7.580794	7.432655	76.C	2.405942	9.399371	1.287747
7.H	5.075885	8.447006	6.884153	77.H	2.834562	10.368963	1.515740
8.C	5.413707	7.182189	8.563600	78.C	2.580001	8.844169	0.018914
9.H	6.282068	7.750012	8.882756	79.H	3.147897	9.380172	-0.734736
10.C	5.027407	6.036508	9.268861	80.C	2.020051	7.596171	-0.276932
11.C	3.912297	5.310798	8.827958	81.C	1.280075	6.909423	0.695693
12.H	3.600674	4.419704	9.365092	82.H	0.838156	5.943891	0.469143
13.C	3.194379	5.715529	7.708561	83.C	1.117312	7.464358	1.960915
14.H	2.331175	5.141067	7.392362	84.H	0.542446	6.942037	2.713763
15.C	5.762261	5.614936	10.510063	85.C	2.272171	6.943070	-1.613128
16.F	5.807742	4.251720	10.650583	86.F	1.193923	6.228687	-2.055364
17.F	5.164272	6.099446	11.655168	87.F	3.325651	6.051290	-1.534958
18.F	7.056408	6.066631	10.531171	88.F	2.594549	7.842679	-2.588304

SUPPORTING INFORMATION

Table S9. Cartesian coordinates and ADF total electronic and Gibbs energies (in parentheses and in kcal mol⁻¹) of compounds **3-X** under analysis computed at the ZORA-BLYP(D3BJ)/TZ2P level of theory in benzene.**3-H (-6736.8, -6540.5)**

C	0.167970	7.064558	4.635863
C	0.814328	7.579374	3.506545
N	4.930368	8.323977	3.704049
H	0.293177	7.625083	2.553189
C	5.331128	9.533666	3.086658
C	4.548420	10.692457	3.239732
H	3.627730	10.647265	3.811437
C	4.961053	11.897185	2.668904
H	4.342797	12.782782	2.795718
C	6.152025	11.971196	1.937960
C	6.938361	10.820988	1.799849
H	7.877414	10.864904	1.253062
C	6.543361	9.613349	2.376090
H	7.173024	8.734891	2.282335
H	6.467797	12.910858	1.492705
C	2.128297	8.042689	3.586006
H	2.623393	8.432102	2.702981
H	-0.856284	6.707503	4.569857
C	5.228274	7.019285	3.241527
C	5.373070	6.757299	1.866337
H	5.273458	7.565293	1.149317
C	5.636607	5.460215	1.425209
H	5.746940	5.275477	0.359186
C	5.737516	4.401168	2.335415
C	5.565194	4.658420	3.700099
H	5.629550	3.846373	4.420580
C	5.313443	5.953243	4.155495
H	5.172865	6.141152	5.214498
H	5.936340	3.391606	1.985845
H	2.718247	7.376571	6.879255
C	0.863941	7.003010	5.849157
N	4.167968	8.427471	4.875624
H	0.384599	6.586606	6.732115
C	4.812410	8.961202	6.018099
C	6.202872	8.813044	6.171988
H	6.771040	8.269150	5.424940
C	6.849603	9.374128	7.273973
H	7.924727	9.248494	7.378120
C	6.129554	10.087223	8.238960
C	4.748190	10.247701	8.076542
H	4.175823	10.816834	8.805455
C	4.091579	9.702417	6.972865
H	3.024975	9.854231	6.845788
H	6.637052	10.519851	9.096987
C	2.181842	7.451752	5.939270
C	2.821124	7.995634	4.809437

3-Me (-8209.4, -7949.5)

H	6.445870	2.352719	2.535949
H	6.628653	2.979801	0.884753
N	4.930921	8.311792	3.700084
H	5.035782	2.494329	1.477682
C	5.320537	9.528170	3.089412
C	4.543855	10.686533	3.264453
H	3.632052	10.638873	3.850447
C	4.951349	11.897781	2.705289
H	4.333504	12.780836	2.858534
C	6.132081	12.002757	1.953769
C	6.907005	10.841329	1.802348
H	7.842857	10.890670	1.248317
C	6.522555	9.625042	2.365703
H	7.157423	8.752296	2.252913
C	6.545982	13.311298	1.317205
H	6.180446	14.167920	1.894030
H	6.138545	13.402792	0.300441
H	7.636261	13.389129	1.239834

3-OMe (-8752.34, -8484.6)

C	0.265705	7.126551	4.508876
C	0.953079	7.638049	3.396324
N	5.091267	8.208830	3.694238
H	0.438343	7.698030	2.440920
C	5.530373	9.379216	3.028681
C	4.805986	10.574878	3.139046
H	3.890247	10.596384	3.720031
C	5.255610	11.749867	2.526496
H	4.668289	12.654416	2.638902
C	6.442629	11.743319	1.782741
C	7.181215	10.552557	1.681587
H	8.113339	10.557064	1.122652
C	6.740397	9.391307	2.305394
H	7.336576	8.487553	2.234763
H	6.158868	14.414498	2.265736
C	2.270522	8.064707	3.514739
H	2.789866	8.449330	2.643528
H	-1.852039	6.897906	6.222454
C	5.329912	6.878063	3.268650
C	5.434059	6.551405	1.908932
H	5.349741	7.330141	1.157917
C	5.646564	5.230232	1.500363
H	5.727954	5.018210	0.440049
C	5.727541	4.205584	2.453549
C	5.591777	4.522754	3.814933

SUPPORTING INFORMATION

C	2.119862	8.029381	3.610082	C	6.174481	10.018503	8.229269
H	2.599834	8.420952	2.719766	C	4.790558	10.187041	8.088482
Br	-1.635588	6.424963	4.578661	H	4.230220	10.746138	8.831127
C	5.218736	7.016397	3.225300	C	4.126170	9.653690	6.989099
C	5.349369	6.766340	1.846999	H	3.058604	9.808362	6.879839
H	5.241624	7.576814	1.134087	C	6.897756	10.641260	9.389735
C	5.610987	5.477457	1.382776	F	7.337876	11.919824	9.100907
H	5.711372	5.295331	0.317500	F	8.011997	9.931343	9.758260
C	5.718505	4.427106	2.295860	F	6.107511	10.754314	10.504347
C	5.561976	4.648434	3.664496	C	2.834765	7.968222	4.830404
H	5.636268	3.826122	4.369016	C	2.217508	7.411297	5.966776
C	5.314439	5.941415	4.126771	H	2.767207	7.324210	6.897321
H	5.186324	6.112949	5.190098	C	0.906227	6.957532	5.895820
Br	6.074911	2.637786	1.651453	H	0.442491	6.525665	6.777702
H	2.738545	7.353355	6.895884	C	0.194655	7.030064	4.689021
C	0.879221	6.983249	5.890015	C	0.814251	7.559245	3.551866
N	4.172923	8.412041	4.880190	H	0.275765	7.612466	2.611631
H	0.403281	6.564138	6.770915	C	2.125294	8.023715	3.618689
C	4.820993	8.954321	6.016274	H	2.600147	8.423831	2.729929
C	6.211569	8.809883	6.167382	C	-1.231745	6.560007	4.649216
H	6.782983	8.260443	5.426937				
C	6.869250	9.379401	7.258123				
H	7.942669	9.260802	7.365976				
C	6.135072	10.093593	8.205570				
C	4.756335	10.261439	8.066618				
H	4.194024	10.837102	8.795030				
C	4.104156	9.702794	6.967507				
H	3.036966	9.856101	6.848112				
Br	7.041654	10.876592	9.724968				
C	2.197485	7.433522	5.959033				
C	2.825895	7.980492	4.825185				

3-CF₃ (-8320.0, -8120.5)

F	6.627470	2.239771	2.672198
F	6.649610	2.993097	0.600049
N	4.925503	8.310348	3.698743
F	4.755045	2.360431	1.523398
C	5.332860	9.524050	3.098576
C	4.564641	10.687385	3.280464
H	3.647150	10.646981	3.856666
C	4.982294	11.895526	2.730520
H	4.378613	12.785540	2.875562
C	6.172167	11.963317	1.995707
C	6.947183	10.807874	1.824185
H	7.882961	10.854918	1.276119
C	6.540063	9.599927	2.379302
H	7.162862	8.719654	2.266034
C	6.598453	13.253059	1.353552
F	6.098904	14.355173	1.995459
F	6.168249	13.343956	0.041923
F	7.962724	13.395439	1.313278
C	5.213452	7.012043	3.219415
C	5.348487	6.769988	1.840155
H	5.244554	7.584175	1.131701
C	5.606779	5.483688	1.378606
H	5.710241	5.309974	0.312276
C	5.717240	4.417033	2.280618
C	5.550115	4.649814	3.651694
H	5.625020	3.828962	4.357838
C	5.301407	5.935675	4.120349
H	5.173340	6.106088	5.183305
C	5.943774	3.020327	1.775261
F	-1.719396	6.437943	3.377342
F	-2.079789	7.427370	5.311700
N	4.179146	8.402852	4.881596
F	-1.395842	5.338418	5.260240
C	4.837796	8.925792	6.018187
C	6.230143	8.777845	6.150446
H	6.792813	8.240567	5.395302
C	6.890390	9.321850	7.247304
H	7.963839	9.192975	7.342634

SUPPORTING INFORMATION

Table S10. Cartesian coordinates and ADF total electronic and Gibbs (in parentheses and in kcal mol⁻¹) of compounds of the potential steps for the formation of **3-Me** from **1-Me** computed at the ZORA-BLYP(D3BJ)/TZ2P level of theory in benzene. R = 4-Me-C₆H₄.

³ [Bi(NR ₂)] (-4150.7, -4031.5)		
Bi	3.367523	10.390514
H	2.375266	5.660026
H	3.108540	7.072140
N	1.555927	9.729443
C	0.271113	10.016131
C	0.006400	9.966116
H	0.787140	9.626130
C	-1.248510	10.319905
H	-1.421285	10.267575
C	-2.292802	10.714106
C	-2.028467	10.749113
H	-2.815133	11.058756
C	-0.779059	10.415151
H	-0.597974	10.469647
C	-3.657044	11.083775
H	-4.437326	10.427954
H	-3.926566	12.112579
H	-3.686818	11.005357
C	1.695794	9.027530
C	2.732552	9.334119
H	3.386950	10.177468
C	2.910949	8.588337
H	3.720927	8.853402
C	2.056771	7.526766
C	1.012660	7.232318
H	0.335292	6.408425
C	0.832940	7.956093
H	0.030411	7.693371
C	2.236929	6.727023
H	1.356887	6.810729
³ [Bi(NR ₂)(benzene)] (-7528.7, -7299.3)		
Bi	0.379322457	1.303900103
H	-5.618635564	-2.073212406
H	-4.904878136	-1.417564174
N	0.054163799	-0.872867705
C	0.975237732	-1.852395691
C	1.154764189	-3.043943785
H	0.523025981	-3.238816854
C	2.157475743	-3.952056710
H	2.276533426	-4.851751280
C	3.028711086	-3.726906252
C	2.836128068	-2.550864715
H	3.479322112	-2.346872817
C	1.829368327	-1.642752294
H	1.695075476	-0.751217230
C	4.122685510	-4.709029737
H	5.108462390	-4.225849088
H	3.968929509	-5.132339808
H	4.156605274	-5.539838557
C	-1.084345738	-1.220840545
C	-1.443901050	-0.481520642
H	-0.789556642	0.318752717
C	-2.620724643	-0.767174046
H	-2.877169363	-0.171327047
C	-3.469812158	-1.809131935
C	-3.093974907	-2.562427141
H	-3.736942431	-3.373441914
C	-1.931504841	-2.277834739
H	-1.674419644	-2.856504438
C	-4.745237048	-2.122514493
H	-4.720056257	-3.135293353
C	-3.236799591	0.868657652
C	-2.874394663	2.052235258
C	-2.778682211	3.248255689
C	-3.046983030	3.259590190
C	-3.410408777	2.075519536
C	-3.506113491	0.880138557
H	-3.297330247	-0.063849881
H	-2.657567472	2.040805425
H	-2.492292986	4.167249392
H	-2.967572663	4.187637461
H	-3.604484496	2.077472787
C	-3.769909895	-0.040281047
C	3.919632482	0.737611472
C	3.591078720	1.906252167
C	2.602566580	1.874375813
C	1.944311024	0.673461198
C	2.273396767	-0.492543662
C	3.262394471	-0.462461434
H	4.680775607	0.764079954
H	4.098853625	2.839704559
H	2.342062629	2.782518747
C	1.171245204	0.648430982
H	1.746819260	-1.419616233
C	3.500487564	-1.365139167
[Bi ₂ (NR ₂) ₄] (-16614.9, -16092.4)		
Bi	-1.253886431	-0.039059629

SUPPORTING INFORMATION

H	-8.737276	1.491697	-1.714101
C	-0.762606	0.347467	-2.426526
C	-0.501507	1.725703	-2.270298
H	-1.192562	2.338253	-1.702077
C	0.604464	2.316112	-2.891679
H	0.769777	3.384745	-2.768218
C	1.490989	1.565348	-3.685702
C	1.233330	0.187606	-3.820630
H	1.917722	-0.428556	-4.399802
C	-3.667911	-2.815345	1.038849
C	0.135647	-0.412871	-3.209781
H	-0.032128	-1.479703	-3.315497
C	2.661165	2.211573	-4.391824
H	3.314822	1.456587	-4.839886
H	3.260198	2.819745	-3.706451
H	2.315029	2.872487	-5.197411
C	-2.656144	-1.147671	-2.611662
C	-3.221482	-0.669968	-3.812145
H	-3.023418	0.354444	-4.113730
C	-4.034158	-1.490594	-4.590025
C	-4.547407	-3.801780	0.542596
H	-4.462429	-1.095667	-5.510162
C	-4.327765	-2.811252	-4.202030
C	-3.753769	-3.281529	-3.013741
H	-3.951396	-4.298854	-2.684429
C	-2.922660	-2.471004	-2.237444
H	-2.482645	-2.873202	-1.335449
C	-5.249137	-3.679438	-5.030329
H	-5.147588	-4.735953	-4.760971
H	-5.039928	-3.576334	-6.101618
H	-6.300126	-3.397818	-4.877052
H	-5.445063	-3.506931	0.011834
C	-3.314020	2.112089	1.978291
C	-2.619535	1.588525	3.086833
H	-1.770143	0.926938	2.940356
C	-2.945392	1.957989	4.390981
H	-2.371317	1.535813	5.213191
C	-3.958917	2.888134	4.657519
C	-4.644937	3.421511	3.552252
H	-5.447597	4.139006	3.717895
C	-4.342231	3.045054	2.246097
H	-4.915964	3.451170	1.419696
C	-4.263293	-5.158983	0.711448
C	-4.272363	3.334557	6.068762
H	-5.347124	3.502956	6.205069
H	-3.763571	4.278523	6.311771
H	-3.947708	2.589169	6.802995
C	-3.342042	2.501352	-0.438524
C	-2.889456	3.835617	-0.486821
H	-2.372050	4.247553	0.373736
C	-3.095271	4.617287	-1.622230
H	-2.731196	5.643371	-1.634890
C	-3.745722	4.099674	-2.756351
H	-4.959444	-5.891296	0.305217
C	-4.214216	2.779270	-2.690742
H	-4.743999	2.355709	-3.542136
C	-4.029530	1.993987	-1.552442
H	-4.419846	0.985011	-1.523792
C	-3.911237	4.928340	-4.011002
H	-4.822158	4.651984	-4.553664
H	-3.064660	4.777544	-4.695702
H	-3.958908	5.998349	-3.780624
C	-3.106119	-5.605120	1.368818

SUPPORTING INFORMATION

References

- [1] N. Abla, S. Bashyam, S. A. Charman, B. Greco, P. Hewitt, M. B. Jimenez-Diaz, K. Katneni, H. Kubas, D. Picard, Y. Sambandan, L. Sanz, D. Smith, T. Wang, P. Willis, S. Wittlin, T. Spangenberg, *ACS Med. Chem. Lett.* **2017**, *8*, 1304-1308.
- [2] W. Clegg, N. A. Compton, R. J. Errington, G. A. Fisher, M. E. Green, D. C. R. Hockless, N. C. Norman, *Inorg. Chem.* **1991**, *30*, 4680-4682.
- [3] A. K. King, A. Buchard, M. F. Mahon, R. L. Webster, *Chem. Eur. J.* **2015**, *21*, 15960-15963.
- [4] S. Molitor, J. Becker, V. H. Gessner, *J. Am. Chem. Soc.* **2014**, *136*, 15517-15520.
- [5] J. W. Dube, Y. Zheng, W. Thiel, M. Alcarazo, *J. Am. Chem. Soc.* **2016**, *138*, 6869-6877.
- [6] S. Stoll, A. Schweiger, *J. Magn. Reson.* **2006**, *178*, 42-55.
- [7] W. Clegg, N. A. Compton, R. J. Errington, N. C. Norman, N. Wishart, *Polyhedron* **1989**, *8*, 1579-1580.
- [8] C. Janiak, *J. Chem. Soc., Dalton Trans.* **2000**, 3885-3896.
- [9] a) C. Hering-Junghans, A. Schulz, M. Thomas, A. Villinger, *Dalton Trans.* **2016**, *45*, 6053-6059; b) R. J. Schwamm, C. M. Fitchett, M. P. Coles, *Chem. Asian J.* **2019**, *14*, 1204-1211; c) D. Michalik, A. Schulz, A. Villinger, *Angew. Chem. Int. Ed.* **2010**, *49*, 7575-7577; d) D. Dange, A. Davey, J. A. B. Abdalla, S. Aldridge, C. Jones, *Chem. Commun.* **2015**, *51*, 7128-7131; e) C. Hering-Junghans, M. Thomas, A. Villinger, A. Schulz, *Chem. Eur. J.* **2015**, *21*, 6713-6717; f) J. Bresien, A. Schulz, M. Thomas, A. Villinger, *Eur. J. Inorg. Chem.* **2019**, *2019*, 1279-1287; g) J. Bresien, C. Hering-Junghans, A. Schulz, M. Thomas, A. Villinger, *Organometallics* **2018**, *37*, 2571-2580; h) N. Burford, C. L. B. Macdonald, K. N. Robertson, T. S. Cameron, *Inorg. Chem.* **1996**, *35*, 4013-4016; i) U. Wirringa, H. W. Roesky, M. Noltemeyer, H.-G. Schmidt, *Inorg. Chem.* **1994**, *33*, 4607-4608; j) S. C. James, N. C. Norman, A. G. Orpen, M. J. Quayle, U. Weckemann, *J. Chem. Soc., Dalton Trans.* **1996**, 4159-4161.
- [10] W. J. Evans, D. B. Rego, J. W. Ziller, *Inorg. Chim. Acta* **2007**, *360*, 1349-1353.
- [11] a) T. A. Hanna, *Coord. Chem. Rev.* **2004**, *248*, 429-440; b) T. A. Hanna, A. L. Rieger, P. H. Rieger, X. Wang, *Inorg. Chem.* **2002**, *41*, 3590-3592; c) X. Kou, X. Wang, D. Mendoza-Espinosa, L. N. Zakharov, A. L. Rheingold, W. H. Watson, K. A. Brien, L. K. Jayarama, T. A. Hanna, *Inorg. Chem.* **2009**, *48*, 11002-11016; d) C. Limberg, *Angew. Chem. Int. Ed.* **2003**, *42*, 5932-5954.
- [12] a) R. B. Licht, D. Vogt, A. T. Bell, *J. Catal.* **2016**, *339*, 228-241; b) Z. Zhai, A. B. Getsoian, A. T. Bell, *J. Catal.* **2013**, *308*, 25-36.
- [13] C. D. T. Nielsen, J. Burés, *Chem. Sci.* **2019**, *10*, 348-353.
- [14] M. C. Ryan, J. R. Martinelli, S. S. Stahl, *J. Am. Chem. Soc.* **2018**, *140*, 9074-9077.
- [15] H. Schumann, *J. Organomet. Chem.* **1986**, *299*, 169-178.
- [16] L. Wu, V. T. Annibale, H. Jiao, A. Brookfield, D. Collison, I. Manners, *Nat. Commun.* **2019**, *10*, 2786.
- [17] W.-W. DuMont, S. Kubiniok, T. Severengiz, *1985*, *531*, 21-25.
- [18] V. P. Böhm, M. Brookhart, *Angew. Chem. Int. Ed. Engl.* **2001**, *40*, 4694-4696.
- [19] K. Schwedtmann, R. Schoemaker, F. Hennersdorf, A. Bauzá, A. Frontera, R. Weiss, J. J. Weigand, *Dalton Trans.* **2016**, *45*, 11384-11396.
- [20] K. Issleib, M. Hoffmann, *Chem. Ber.* **1966**, *99*, 1320-1324.
- [21] D. L. Dodds, M. F. Haddow, A. G. Orpen, P. G. Pringle, G. Woodward, *Organometallics* **2006**, *25*, 5937-5945.
- [22] S. Zhang, H. Neumann, M. Beller, *Chem. Eur. J.* **2018**, *24*, 67-70.
- [23] V. K. Gupta, L. K. Krannich, C. L. Watkins, *Inorg. Chim. Acta* **1988**, *150*, 51-55.
- [24] a) S. Greenberg, D. W. Stephan, *Chem. Soc. Rev.* **2008**, *37*, 1482-1489; b) R. Waterman, *Curr. Org. Chem.* **2008**, *12*, 1322-1339; c) J. D. Masuda, A. J. Hoskin, T. W. Graham, C. Beddie, M. C. Fermin, N. Etkin, D. W. Stephan, *Chem. Eur. J.* **2006**, *12*, 8696-8707; d) L.-B. Han, T. D. Tilley, *J. Am. Chem. Soc.* **2006**, *128*, 13698-13699; e) M. C. Fermin, D. W. Stephan, *J. Am. Chem. Soc.* **1995**, *117*, 12645-12646; f) R. Waterman, *Organometallics* **2007**, *26*, 2492-2494.
- [25] F. A. Neugebauer, P. H. H. Fischer, *Chem. Ber.* **1965**, *98*, 844-850.
- [26] a) G. te Velde, F. M. Bickelhaupt, E. J. Baerends, C. Fonseca Guerra, S. J. A. van Gisbergen, J. G. Snijders, T. Ziegler, *J. Comput. Chem.* **2001**, *22*, 931-967; b) R. J. Schwamm, M. Lein, M. P. Coles, C. M. Fitchett, *Chem. Commun.* **2018**, *54*, 916-919.
- [27] a) A. D. Becke, *Phys. Rev. A* **1988**, *38*, 3098-3100; b) C. Lee, W. Yang, R. G. Parr, *Phys. Rev. B* **1988**, *37*, 785-789; c) B. G. Johnson, P. M. W. Gill, J. A. Pople, *J. Chem. Phys.* **1993**, *98*, 5612-5626; d) S. Grimme, S. Ehrlich, L. Goerigk, *J. Comput. Chem.* **2011**, *32*, 1456-1465; e) T. V. Russo, R. L. Martin, P. J. Hay, *J. Chem. Phys.* **1994**, *101*, 7729-7737; f) S. Grimme, J. Antony, S. Ehrlich, H. Krieg, *J. Chem. Phys.* **2010**, *132*, 154104.
- [28] a) E. v. Lenthe, E. J. Baerends, J. G. Snijders, *J. Chem. Phys.* **1994**, *101*, 9783-9792; b) E. van Lenthe, R. van Leeuwen, E. J. Baerends, J. G. Snijders, *Int. J. Quantum Chem.* **1996**, *57*, 281-293.
- [29] a) A. Klamt, G. Schüermann, *J. Chem. Society, Perkin Trans. 2* **1993**, 799-805; b) A. Klamt, *J. Phys. Chem.* **1995**, *99*, 2224-2235.
- [30] a) F. M. Bickelhaupt, A. Diefenbach, S. P. de Visser, L. J. de Koning, N. M. M. Nibbering, *J. Phys. Chem. A* **1998**, *102*, 9549-9553; b) F. M. Bickelhaupt, E. J. Baerends, in *Rev. Comput. Chem.*, Vol. 15 (Eds.: K. B. Lipkowitz, D. B. Boyd), Wiley-VCH, New York, **2000**, pp. 1-86; c) L. P. Wolters, F. M. Bickelhaupt, *WIREs Comput. Mol. Sci.* **2015**, *5*, 324-343.

Author Contributions

Synthesis: K. O. (exclusively)**X-ray diffraction analyses:** J. R., A. H., C. L. (equal)**EPR spectroscopy:** I. K. (lead); K. O., C. L. (supporting)**DFT calculations:** J. P. (lead); F. M. B., C. L. (supporting)**Composition of the manuscript:** K. O., C. L. (lead); J. P. (supporting)**Discussion of results and correction of manuscript:** all authors**Project administration:** C. L. (lead)**Acquisition of funding:** K. O., J. P., F. M. B., C. L.

Conflicts of Interest

The authors declare no conflicts of interest

Acknowledgements

We thank Hannah Dengel, Benedikt Ritschel, and Dr. Conor Pranckevicius for their contributions. Financial support by the FCI, the DFG, the University of Würzburg, the Cusanuswerk, the Netherlands Organisation of Scientific Research (NWO), and the Spanish Government (PID2019-106830GB-I100 and MDM-2017-0767) is gratefully acknowledged. This project has received funding from the European Research Council (ERC) under the European Union's Horizon 2020 research and innovation program (grant agreement No946184). C. L. thanks Prof. Holger Braunschweig for continuous support.